SIMULATION STUDY OF A GAS CONDENSATE WELL TEST

by

Nasser AL-Mohannadi

A thesis submitted to the faculty and the Board of Trustees of the Colorado School of Mines in partial fulfillment of the requirements for the degree of Master of Science (Petroleum Engineering).

Golden, Colorado

Date March 10, 2000

Signed: _____
Nasser Al-Mohannadi

Approved: _____
Dr. John R. Fanchi
Thesis Advisor

Golden, Colorado

Date March 10, 2000

_____
Dr. Craig W. Van Kirk
Professor and Head,
Department of
Petroleum Engineering

ABSTRACT

The primary objective of a reservoir study is to predict the performance of a reservoir and find ways to increase ultimate recovery. One objective of reservoir simulation is to evaluate the effects of altered operating conditions on the recovery. For example, simulation can forecast changes in recovery resulting from different well patterns and spacing, variations in relative permeability, and changes in well completion intervals. It is widely known that gas condensate reservoir performance can be affected by the presence of hydrocarbon liquids arising from retrograde condensation.

The objective of this project is to conduct a simulation study of a gas condensate well test using a commercial simulator (ECLIPSE 100/200) and data obtained from private industry. This simulation study includes: (1) Model initialization (data preparation) by preparing a fluid property model data from an equation-of-state analysis of fluid property data; (2) History matching a single phase gas condensate well test followed by sensitivity study of relevant factors; and (3) Prediction runs for wellbore pressure both above and below dew point pressure. The prediction runs assess the effect of two phase flow on model performance; and are compared with different grid representations and different relative permeability models.

From the model initialization, it is found that the Peng-Robinson EOS gives a very good match for the gas condensate laboratory data.

Based on the history match obtained in this study, it is found that matching the pressure transient test has some restrictions because of its short period and lack of geological information. It is concluded that data from different well tests with different durations of the tests for the same well can give different history matching results. It is found during the sensitivity runs that the location and properties of a seal fault to form a wedge can affect the match results. It is concluded also that different local grid refinement (LGR) give the same results for this problem. In the prediction runs, it is found that different relative permeabilities to gas give different pressure behavior and Cartesian local grid refinement (LGR) is less sensitive compared to Radial LGR during two-phase flow.

Based on this study, it is recommended that field data be collected and matched. More information would be obtained by attempting to match field performance when two phases are flowing.

A preliminary review of compositional data from samples taken at different depths suggests that a compositional gradient may exist in the field. Further study of the compositional gradient could be performed using PVT and compositional data for well #1 from different depths.

TABLE OF CONTENTS

LIST OF FIGURES

LIST OF TABLES

NOMENCLATURE

a_M and b_M = molar weighted averages for equations of state

B = formation volume factor

k = effective permeability

k_{rw} = relative permeability to water

k_{rg} = relative permeability to gas

k_{row} = relative permeability to oil in water-oil system

k_{rog} = relative permeability to gas in oil-gas system

$k_{rg(Sorg)}$ = relative permeability to gas at residual oil saturation

K_{ij} = binary interaction coefficients obtained from experimental data on two-component interaction systems.

P_{ws} = shut-in pressure

P_c = critical pressure

$\hat{q}_s$ = injected or produced rate

R = gas constant

S = saturation

S_{wi} = irreducible water saturation

S_{gc} = critical gas saturation

S_{orw} = residual oil saturation in water-oil system

S_{org} = residual oil saturation in gas-oil system

t = shut-in time

T_c = critical temperature

T_r = reduced temperature

ϕ = porosity

μ = viscosity

Ω_a and Ω_b = constants for equations of state

ACKNOWLEDGMENT

I would like to thank first the GOD for helping, guiding and giving me patience in this work. Also, I would like to thank the academic members of the Petroleum Engineering Department for their help, especially my advisor Dr. John Fanchi and Dr. Erdal Ozkan. I would like to thank EOG Resources for providing the data used in this study.

DEDICATION

I dedicate this work to my father and mother and to all of my family members.

Chapter 1

INTRODUCTION

The primary objective of a reservoir study is to predict the performance of a reservoir and find ways to increase ultimate recovery. One objective of reservoir simulation is to evaluate the effects of altered operating conditions on the recovery. For example, simulation can forecast changes in recovery resulting from different well patterns and spacing, variations in relative permeability, and changes in well completion intervals. It is widely known that gas condensate reservoir performance can be affected by the presence of hydrocarbon liquids arising from retrograde condensation.

The objective of this project is to conduct a simulation study of a gas condensate well test using a commercial simulator (ECLIPSE 100/200) and data obtained from private industry. This simulation study includes three main parts: model initialization (data preparation), history matching and prediction runs. This report consists of three different chapters representing the three main parts followed by the last chapter of conclusions and recommendations.

1.1 LITERATURE REVIEW

Reservoir simulation has been used since the beginning of petroleum engineering in the 1930's. On the other hand, the potential of simulation was recognized in the late 1940's and early 1950's by a number of companies. They were doing fundamental research on numerical analysis and development of practical methods[1]. Before 1960, engineering calculations consisted largely of analytical methods, zero-dimensional material balances and one-dimensional (1D) Buckly-Leverett calculations[2].

During the 1960's, the term "simulation" became commonly used to describe sophisticated programs. These programs solved large sets of finite-difference equations that describe two- and three-dimensional (2D and 3D), transient, multiphase flow in heterogeneous porous media[2].

Numerical reservoir simulators are used widely because they can solve problems that cannot be solved any other way. Reservoir simulation allows a more detailed study of the reservoir by dividing the reservoir into a number of blocks and applying fundamental equations for flow in porous media to each block.

The simulation model can represent the reservoir as a 2- or 3D network of grid blocks and the simulation model equations are basically the familiar volumetric material balance equation written for each phase for each grid block[2]. **Fig. 1.1** illustrates 1-, 2-, and 3D grids representing a portion of a reservoir. The block and its two or four

neighbors are denoted by B and N in the 1D and 2D grids. The 3D grid has interior blocks with six neighbors, two on either side of the block in the x, y, and z-directions.

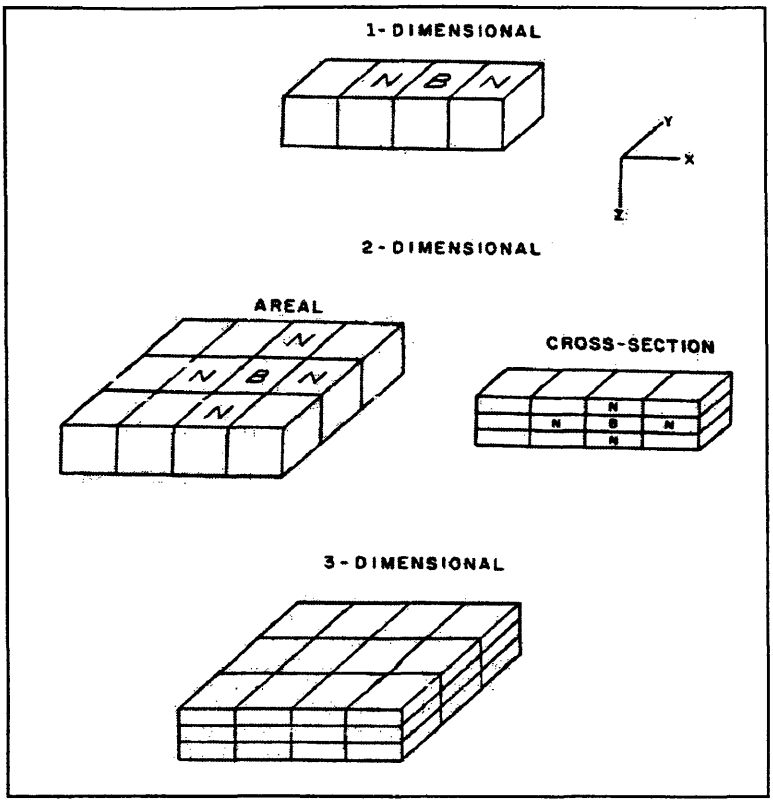

Fig. 1.1 1-, 2-, and 3D grids[2].

A simulation program solves a set of difference equations that are obtained by replacing partial derivatives with finite differences, which are derived from Taylor's series[3,4]. The set of partial differential equations describing multiphase, multidimensional fluid flow in porous media are not amenable to analytical solution. The equations are complicated by such factors as: (1) reservoir heterogeneity, (2) nonlinearity of relative

permeability and capillary pressure, and (3) nonlinearity of fluid PVT properties as a function of pressure, composition and temperature.

The simulator solution procedure is outlines below:

1. Formulate fluid flow equations, such as

$$\frac{\partial}{\partial x}\left[\frac{k}{\mu B}\left(\frac{\partial P}{\partial x}\right)\right]+\hat{q}_s=\frac{\partial}{\partial t}\left(\frac{\phi S}{B}\right) \quad \text{..... (1.1)}$$

2. Replace derivatives with finite differences

   - For grid block length Δx:

$$\frac{\partial P}{\partial x}\approx\frac{P_{i+1}-P_i}{x_{i+1}-x_i}\equiv\frac{\Delta P}{\Delta x} \quad \text{..... (1.2)}$$

   - For time step interval Δt:

$$\frac{\partial S}{\partial t}\approx\frac{S^{n+1}-S^n}{t^{n+1}-t^n}\equiv\frac{\Delta S}{\Delta t} \quad \text{..... (1.3)}$$

3. Numerically solve the resulting set of linear algebraic equations.

There are two widely used techniques to solve the equations numerically: The Newton-Raphson method, and the IMPES method. The Newton-Raphson technique is considered a fully implicit technique because all primary variables are calculated at the same time. Primary variables are pressures and saturations. By contrast, the Implicit

Pressure-Explicit Saturation (IMPES) procedure solves for pressures at the new time level using saturations at the old time level. Then, IMPES uses pressures at the new time level to explicitly calculate saturations at the new time level. A flow chart for a typical simulator is shown in **Fig. 1.2**.

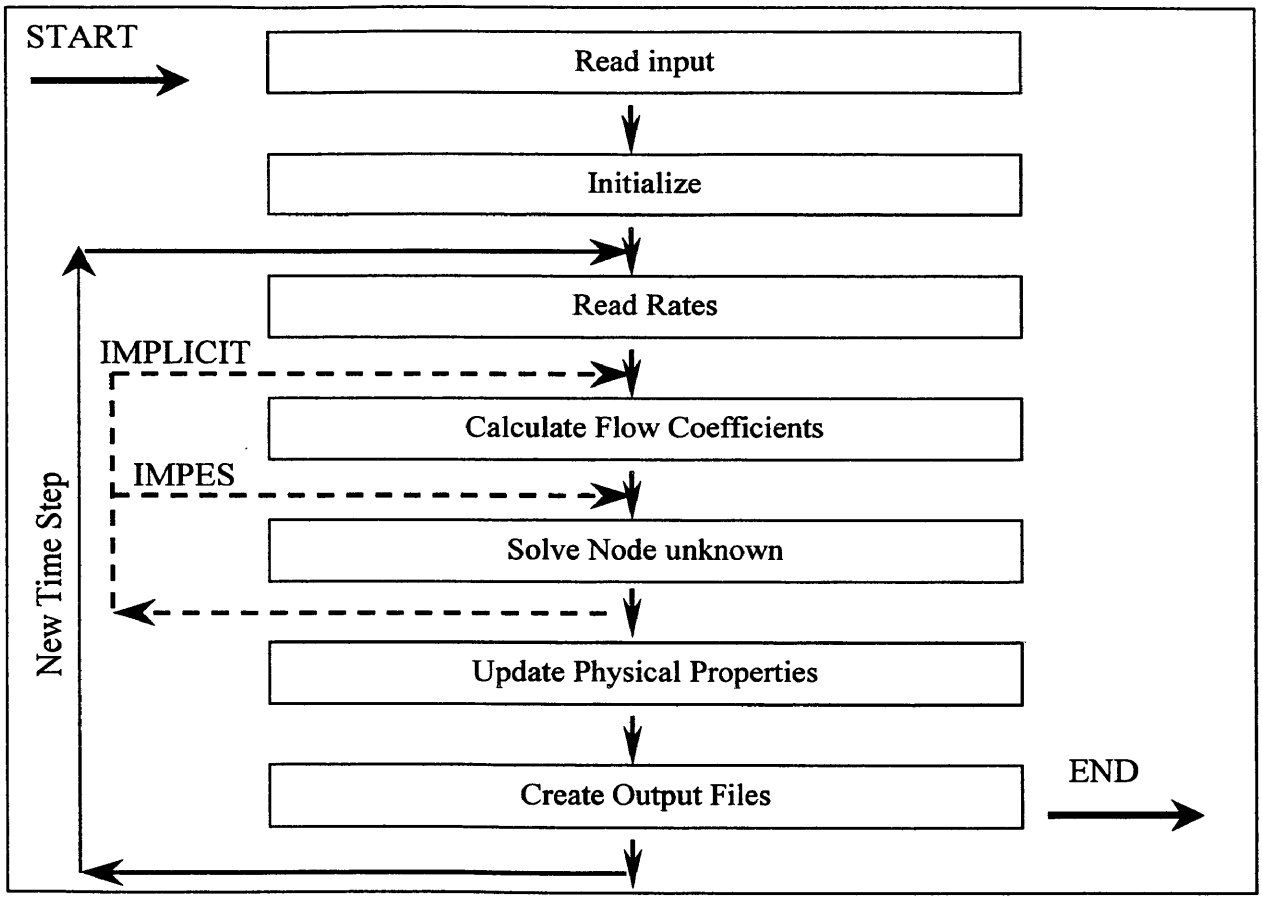

Fig. 1.2 Typical simulator flow chart[3].

The most common simulators in use are black oil and compositional simulators. A compositional simulator represents the fluid as a mixture of hydrocarbon components. A

black oil simulator may be viewed as a compositional simulator with two components. It can have gas dissolved in oil as well as oil dissolved in the gas phase. The selection of reservoir simulator depends on both the nature of the original reservoir fluid and the recovery process of interest. Black oil and compositional simulators assume isothermal flow and instantaneous mass transfer within a block.

The importance of gas condensate reservoirs has grown considerably since the 1930's. The optimum development and operating strategies for these reservoirs are different from crude oil and dry gas reservoirs[2]. The single most important factor about gas condensate systems is that they exist either wholly or predominantly as vapor phase in the reservoir at the time of discovery. A thorough understanding of fluid properties together with a good understanding of the special economics involved is required for optimum engineering of gas condensate reservoirs. Other aspects of a gas condensate reservoir system can significantly influence production performance. They include geological environment, rock properties, well deliverability, well costs and spacing, well-pattern geometry, and plant costs. Some of these factors play a role in the following analysis.

There is a large literature on gas condensate reservoirs. Articles have addressed many different models and correlations for the purpose of predicting the multiphase flow of hydrocarbon mixtures. New methods are presented for modeling pressure loss in retrograde gas-condensate wells. These methods employ redefined flow pattern map boundaries based upon the utilization of available well test data and are superior in

accuracy to existing multi phase flow regime. A study was conducted to evaluate the accuracy of the existing multiphase flow pressure loss prediction methods for both crude oil and gas condensate wells[5]. Different crude oil compositions, retrograde gas condensate compositions and well test pressure surveys from a wide range are used to ascertain the suitability of the correlations. It is found that Peng Robinson equation of state with suitably adjusted pseudo-component properties resulted in excellent agreement with crude oil laboratory data at saturation conditions. Likewise, similar success was achieved with Schmidt Wenzel equation of state for retrograde gas condensate mixtures. In this study, Peng Robinson equation of state shows very good match for the gas condensate laboratory data as illustrated in Chapter Two (Model initialization).

One study in the literature focused on applying modern 3D modeling technology to a large gas condensate field[6]. The study found that reservoir modeling and history matching of production and well test data led to a better reservoir description of the gas condensate field and improved reliability of the production prognosis. The 3D compositional model with a dual porosity option showed that the pressure drop in the in fractures fell below the dew point pressure more rapidly than predicted by other studies using a single porosity models. The value of well test data for improving reservoir characterization is also demonstrated in this study described below.

1.2 SCOPE OF THE SIMULATION STUDY

A typical reservoir simulation study involves certain type of activities and procedures. Although the distribution of effort among the activities varies from project to project. **Fig. 1.3** charts the most significant activities in a typical study. Those activities are described briefly below:

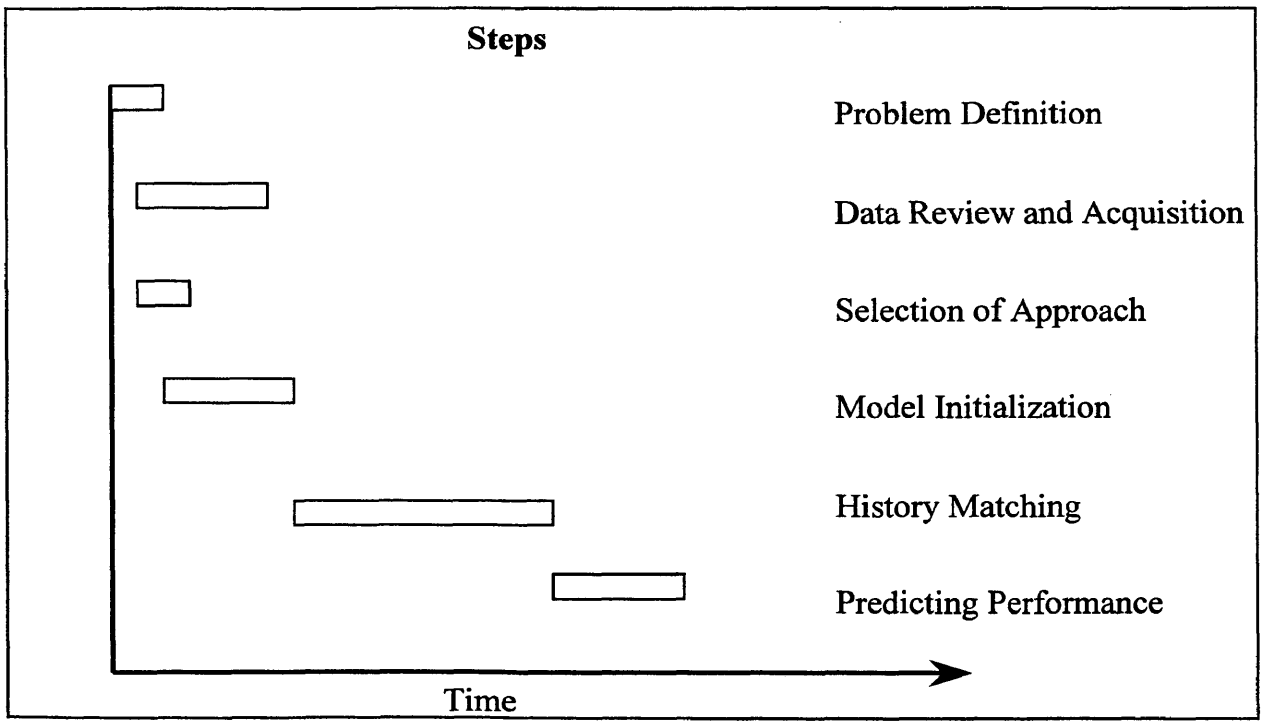

Fig. 1.3 Most common activities in a typical reservoir simulation study.

- Problem Definition

The first step in conducting a study is to define the reservoir performance problem and the associated operating problem. In this study, the type of reservoir is gas condensate. In a dry gas reservoir, it is possible to recover more than 85% of the initial gas in place. In a gas condensate reservoir, it is common to lose as much as 50% to 60% of the liquefiable hydrocarbons as a result of retrograde condensation[7]. This significantly decreases the productivity of very high rate gas wells in many of the world's largest hydrocarbon reservoirs. A widely accepted cause of this decrease in productivity index (PI) is the decrease in gas relative permeability due to the build up of condensate in the near wellbore region[8]. One of the goals of this study is to determine the affect of relative permeability interference on the production performance of a gas condensate well. The behavior of the well is first established by history matching an actual well test.

- Data Review and Acquisition

Acquired data must be evaluated with a focus on its quality and completeness. In this study, data have been provided from a private company and are reviewed later.

- Selection of Approach

Once the reservoir flow problems have been defined, the type of simulation model that is most suitable for solving the flow problem can be chosen. There are three different

types of models: full field models, window area models, and conceptual models[3]. A window area model for an individual well is used in this study because it is designed to look at the behavior of an individual well in a realistic reservoir environment. This means that interference from other wells is not considered.

The selection of a simulator and design of a simulation model are influenced by the type of process to be modeled, the difficulty of the fluid mechanics problem, and the objective of the study. The black oil simulators Eclipse 100 and its extension Eclipse 200 are used in this study. Eclipse 200 includes local grid refinement and other options that are not available in Eclipse 100. Eclipse 100 and 200 are robust programs that use the fully implicit method to solve the finite difference equations.

- Model Initialization

A simulation model requires several types of input data. The groups of input data generally required in making a simulation run are: reservoir description, geological and petrophysical properties, relative permeability and capillary pressure relationship, and fluid properties. Suitable correlations can be used to generate data that are not available. Some correlations are used to generate fluid properties and relative permeability tables. The data preparation is discussed in detail in Chapter Two (Model initialization).

- History Matching

After a reservoir model has been constructed, it must be tested to determine whether it can duplicate field behavior. In this study, the history match is based on matching the pressure build-up test for single phase flow. History matching is discussed in detail in Chapter Three.

- Predicting Performance and Analyzing Results

Once a reasonable history match has been obtained, the model can be used to predict the future performance of the well or reservoir under different operating conditions. Prediction runs are discussed in detail in Chapter Four.

1.3 OBJECTIVE

The objective of this project is to conduct a simulation study of a gas condensate well test using a commercial simulator (ECLIPSE 100/200) and data obtained from private industry. This simulation study includes:

(1) Model initialization (data preparation) by preparing PVT data from an equation-of-state analysis; relative permeability curves are estimated using correlations;

(2) History matching a single phase gas condensate well test followed by sensitivity study of relevant factors; and

(3) Prediction runs for wellbore pressure both above and below dew point pressure. The prediction runs assess the affect of two-phase flow on model performance, and are compared with different grid representations and different relative permeability models.

Chapter 2

MODEL INITIALIZATION

(DATA PREPARTION)

The first step toward obtaining a history match is the collection and analysis of data. A simulation model requires several types of input data. The reservoir description must include reservoir structure, grid representation, and attributes such as porosity and permeability.

Geological and petrophysical work, which involve log and core analyses, provide information about these items. Laboratory tests on core samples yield estimates of relative permeability and capillary pressure relationships. Fluid PVT properties, such as formation volume factors, solution gas, and viscosities are obtained by laboratory tests. Finally, well locations, perforated intervals, and productivity indices (PI's) must be specified.

Proper testing of gas condensate wells is important to plan the best production and recovery program for the reservoir. Well tests and samples make it possible to accurately determine fluid properties and phase behavior. Fluid properties are then used to estimate hydrocarbon materials in place. In this study, fluid, reservoir and wellbore data were acquired from existing reports provided from a private company.

2.1 RESERVOIR CHARACTERIZATION

A structure map of the field for the well test analyzed in this study is shown in **Fig. 2.1**. It can be seen that the field is bounded by two major faults (Fault I and II). Without evidence to the contrary, we assume that the faults are sealing. Sealing faults are no flow boundaries. This assumption is subject to verification during the history match of the study. Fault III is shown on the west side of the field and is considered a minor fault. Three wells are shown in the figure. Well #1 located near Fault II is the well of interest in this study.

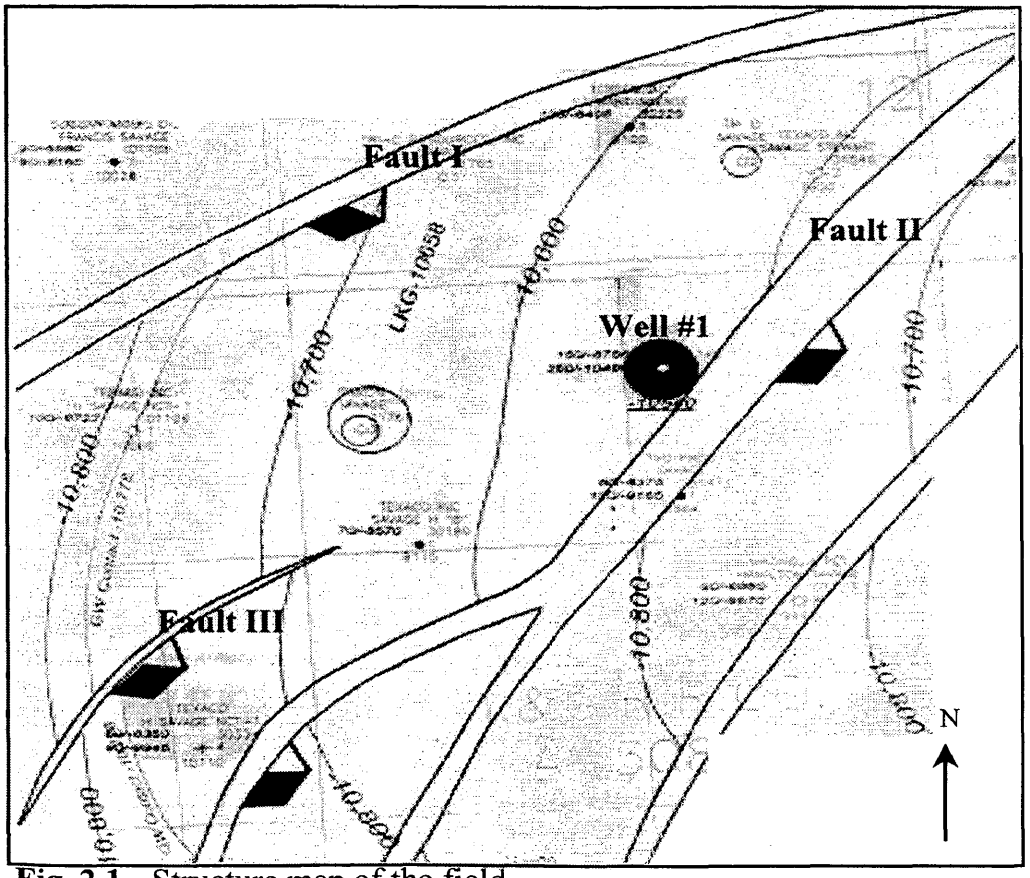

Fig. 2.1 Structure map of the field.

A well log trace for Well #1 is shown in **Fig. 2.2**. An analysis of the well log data shows that two major sands are present and are separated by a shale section. Well log results are presented in **Table 2.1**.

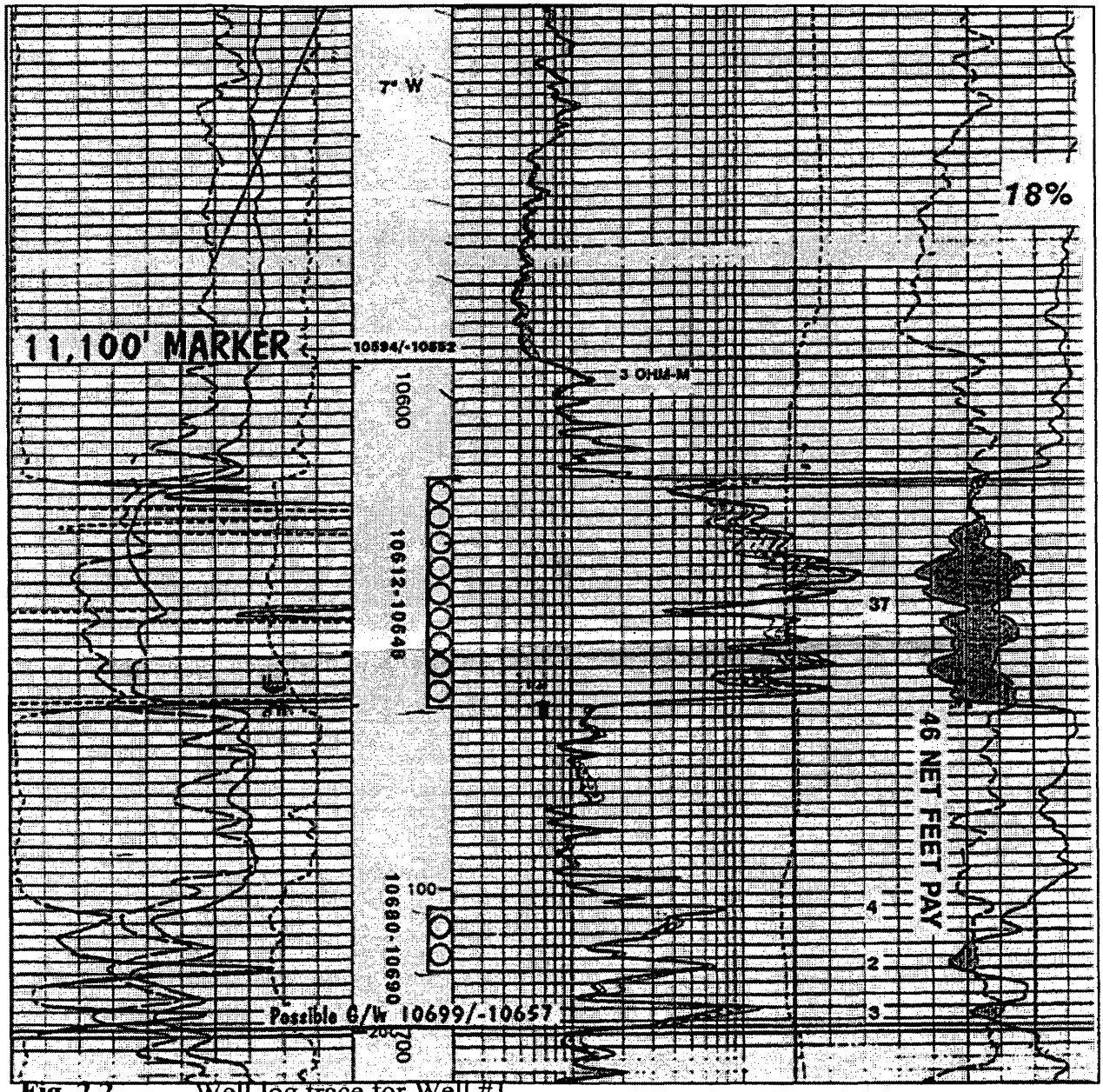

Fig. 2.2 Well log trace for Well #1.

Table 2.1

Well Log Analysis Summary

Litho logy	Depth to top of formation (ft)	Porosity ϕ (fr.)	Water saturation S_w (fr.)	Gross thickness H (ft)
Shale	10582	0.0	0.243	30
Sandstone	10612	0.298	0.243	36
Shale with Sandstone	10648	0.0	0.243	32
Sandstone with Shale	10680	0.298	0.243	10
Sandstone with Shale	10690	0.298	1.0	10

Figure 2.3 shows the structure map with a Cartesian grid displayed over the structure. The dimensions of the grid system are shown in **Table 2.2**.

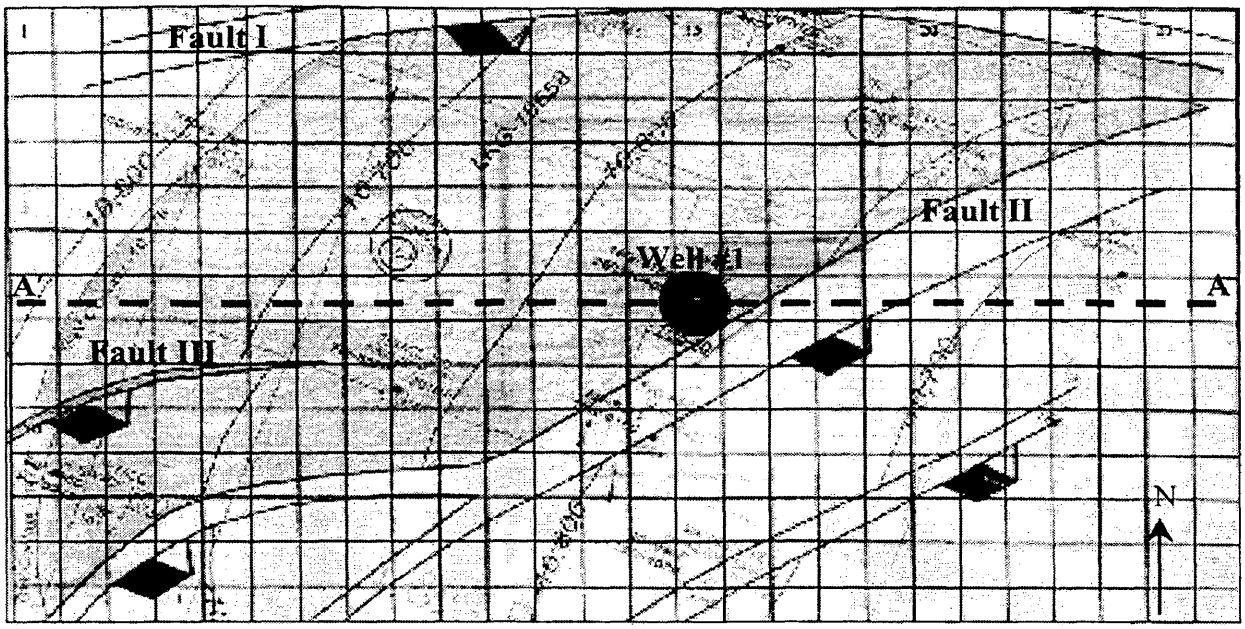

Fig. 2.3 Structure map with Cartesian grid system.

Table 2.2

Grid Dimensions

	X- axis	Y-axis
Number of grid blocks	26	14
Size of single block (ft)	406	406

The cross-section through points A and A′ of the structure map is shown in **Fig. 2.4**.

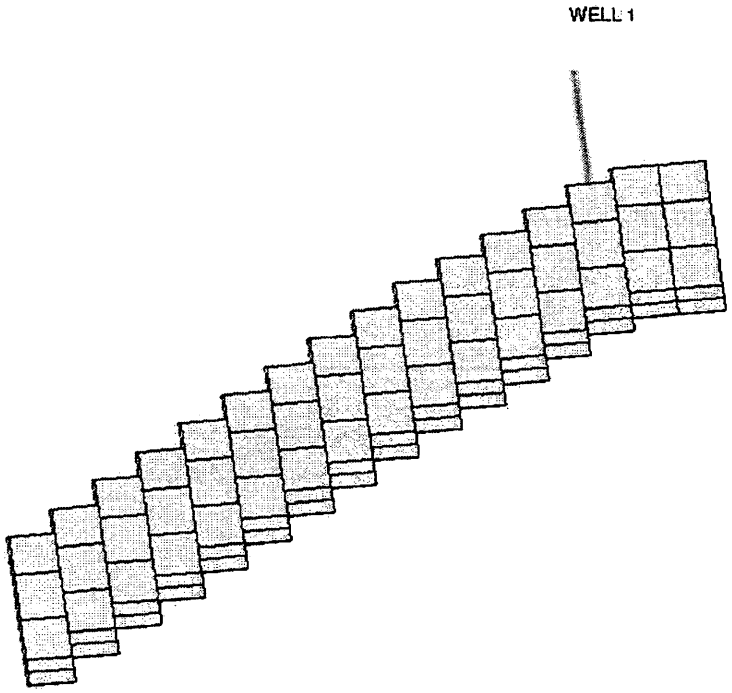

Fig. 2.4 A cross-section through points A and A′ of the structure map.

A schematic cross-section through points A and A′ of the structure map is shown in **Fig. 2.5** for the well block. This figure shows the layering system used in the model. The perforation intervals are shown as vertical dashed lines. The gas-water contact was estimated from well logs and is shown in **Fig. 2.5**.

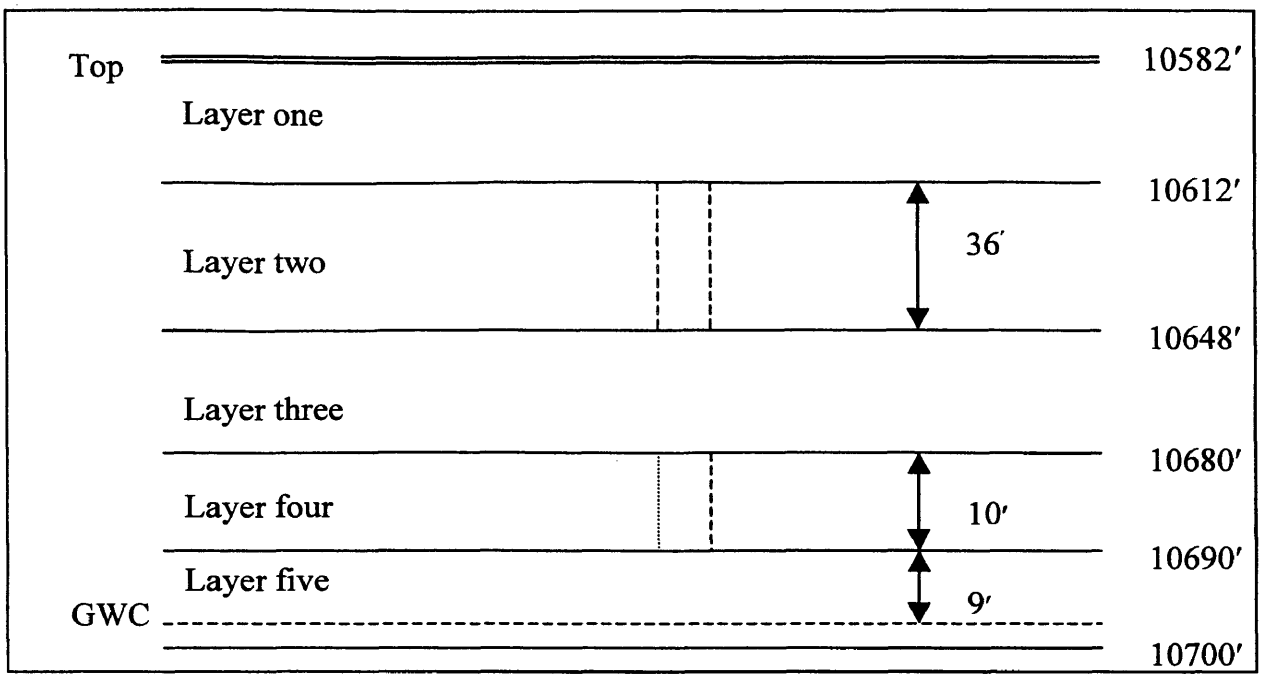

Fig. 2.5 Schematic cross-section of the structure map for the well block.

2.2 POROSITY AND PERMEABILITY

Porosity of 29.8 % was obtained from the well log analysis summarized in **Table 2.1**. The permeability is found from well test analysis. **Table 2.3** shows values of permeability estimated from different build-up tests.

Table 2.3

Build-up Test Interpretation Summary

DATE	BOUNDARY	DURATION Hour	PERMEABILITY md.
6/23/98	Faults	24.1	229
9/13/98	Infinite	3.513	665

2.3 FLUID PROPERTIES (PVT DATA)

An EOS (equation of state) was used to determine the volumetric and phase behavior of reservoir fluids and to prepare fluid properties for the simulation. The EOS concept has the following advantages[9]:

- One EOS for representing liquid and vapor phases.
- The EOS provides a single, consistent source for phase property calculations.
- The EOS ensures convergence at the critical point.

The Peng-Robinson[9] (1975) equation of state is given by the following expression:

$$P = \frac{RT}{V-b} - \frac{a\alpha}{(V+b)^2 - cb^2} \quad \text{.....(2.1)}$$

where

$$\alpha = (1 + m(1 - T_r^{0.5}))^2 \quad \text{.....(2.2)}$$

$$a = \Omega_a \frac{R^2 T_c^{\,2}}{p_c} \quad \text{.....(2.3)}$$

$$b = \Omega_b \frac{R\,T_c}{p_c} \quad \text{.....(2.4).}$$

The physical constants and units of variables are:

R = gas constant, 10.73 psia-ft^3/lb-mole-^{o}R

P_c = critical pressure, psia.

T_c = critical temperature, ^{o}R

T_r = reduced temperature, ^{o}R

$\Omega_a = 0.421875$

$\Omega_b = 0.125$

The constant c in **Eq. 2.1** is a whole number optimized by analyzing the Z_c(universal critical gas compressibility factor) and b/V_c(critical volume) values obtained from the equation.

The PVT program provided by Geo-Quest was used to tune the EOS parameters by matching two different sets of lab data obtained from tests on samples taken from Well #1 at different depths and dates. One sample was taken on June 21,1998 and the other on May 18,1998. A description of the reservoir fluid test made on June 21,1998 and a compositional analysis of the well stream used for EOS calculations are shown in **Table 2.4** and **Table 2.5** respectively. The data in **Table 2.4** and **2.5** were used for the compositional simulation study because the fluid sample taken on June 21, 1998 was from the same depth and approximate time as the build-up well test conducted on June 23, 1998 and matched in this study.

Table 2.4

Description of Reservoir Fluid for Test Conducted on June 21,1998

Type of Test	Gas condensate fluid study
Reservoir Fluid Type	Undersaturated Gas
Saturation Conditions:	
Pressure (retrograde Dew Point)	7078 psig
Temperature	255 °F
Reservoir Conditions:	
Pressure	8059 psig
Temperature	255 °F

Table 2.5

Compositional Analysis of Well Stream for Test Conducted on June 21,1998

Component	**Mole %**
Nitrogen	0.466
Carbon Dioxide	1.187
Methane	80.089
Ethane	6.154
Propane	2.672
Iso-butane	1.255
N-butane	0.854
Iso-pentane	0.448
N-pentane	0.345
Hexanes	0.543
Heptanes Plus	5.988
TOTALS	**100.0**

Sensitivity runs were made for different weighting factors of saturation pressure (p_s) and GOR, and with different BIC (binary interaction coefficients). The BIC can be described as follow:

$$a_M = \sum_i \sum_j X_i X_j a_{ij}$$

$$b_M = \sum_i X_i b_i$$

where a_M and b_M are molar weighted averages;

$$a_{ij} = (a_{ii} a_{jj})^{1/2} ((1 - K_{ij})$$

and K_{ij} are the binary interaction coefficients obtained from experimental data on two component interaction systems.

It is found that the best match for the June 21, 1998 data is with a weighting factor applied to the saturation pressure of 3, GOR weighting factor of 1 and with binary interaction coefficients between c1, c2 and c7+ allowed to vary in the EOS regression analysis. The best match for May 18, 1998 data has a saturation pressure weighting factor of 2, GOR weighting factor of 1 and binary interaction coefficients between c1, c2 and c7+ allowed to change. The regression data from EOS for June 21, 1998 data is shown in **Table 2.6** and **Fig. 2.6** below.

Table 2.6

Regression Data from EOS Match for Test Conducted on June 21, 1998

Variable	Laboratory Measured Value	EOS Calculated Value
Dew Point Pressure, psia	7078	7058.4
Gas Oil Ratio (GOR) at 914 psia, Mscf/stb	7.287	7.289
Gas Oil Ratio (GOR) at 14.7 psia, Mscf/stb	0.328	0.328

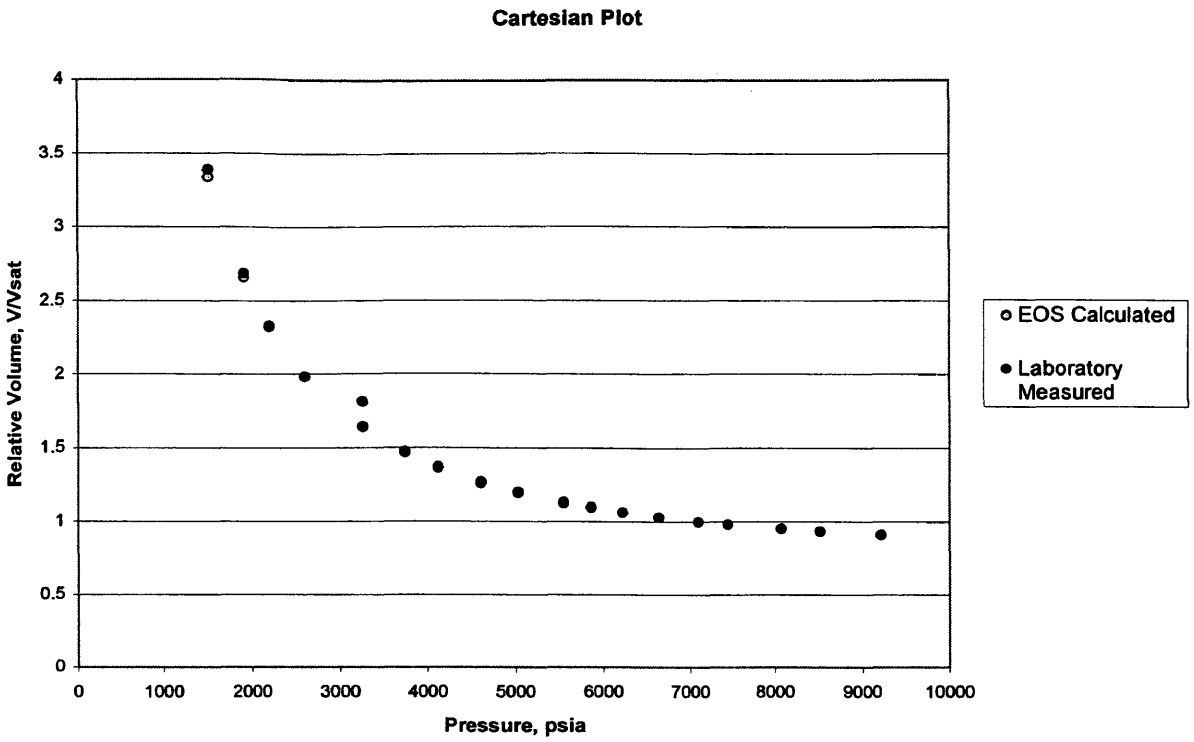

Fig. 2.6 Regression data from EOS match for relative volumes for test conducted on June 21, 1998.

The EOS for June 21, 1998 data was used to prepare black oil data for Eclipse 100 because the depth and the timing of this data more closely matches well test data matched in this study. The calculated black oil data were linearized for the undersaturated part of gas property table (PVTG) and saturated part of the oil property table (PVTO). Black oil data of May 18, 1998 are available for further study, but were not needed in this study. Black oil fluid properties for oil properties and gas properties used in Eclipse 100 are shown in the figures below:

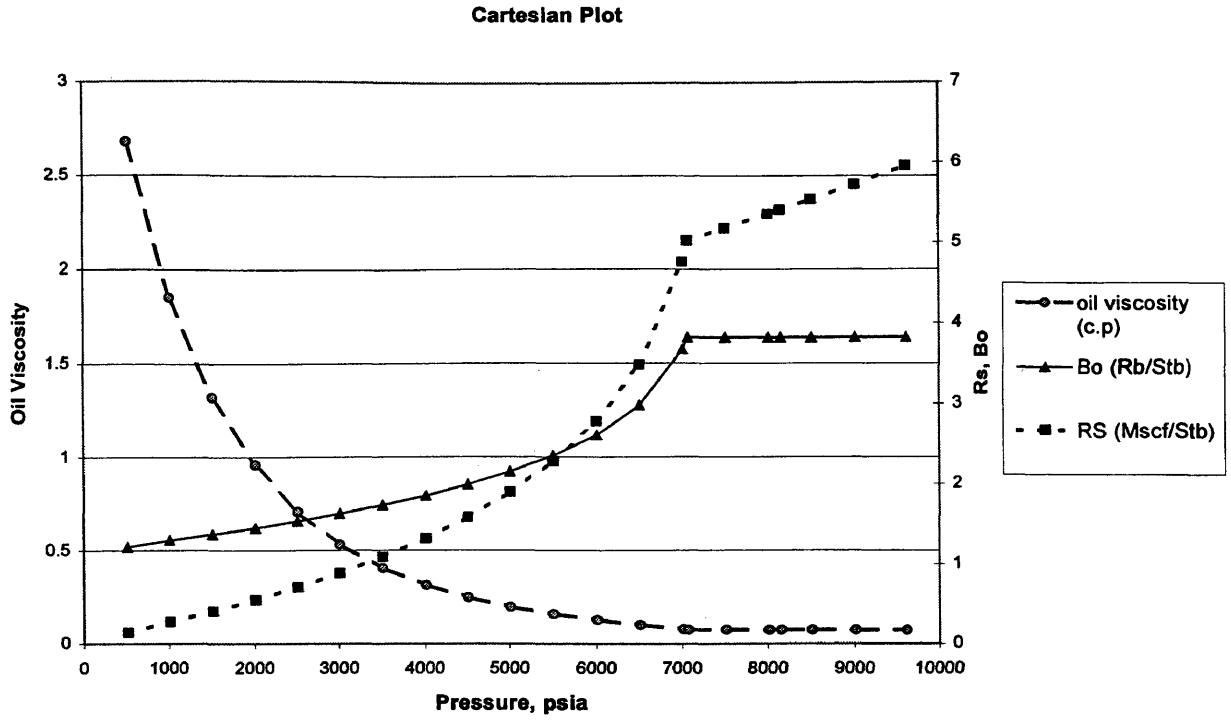

Fig. 2.7 Oil Property data for test conducted on June 21, 1998.

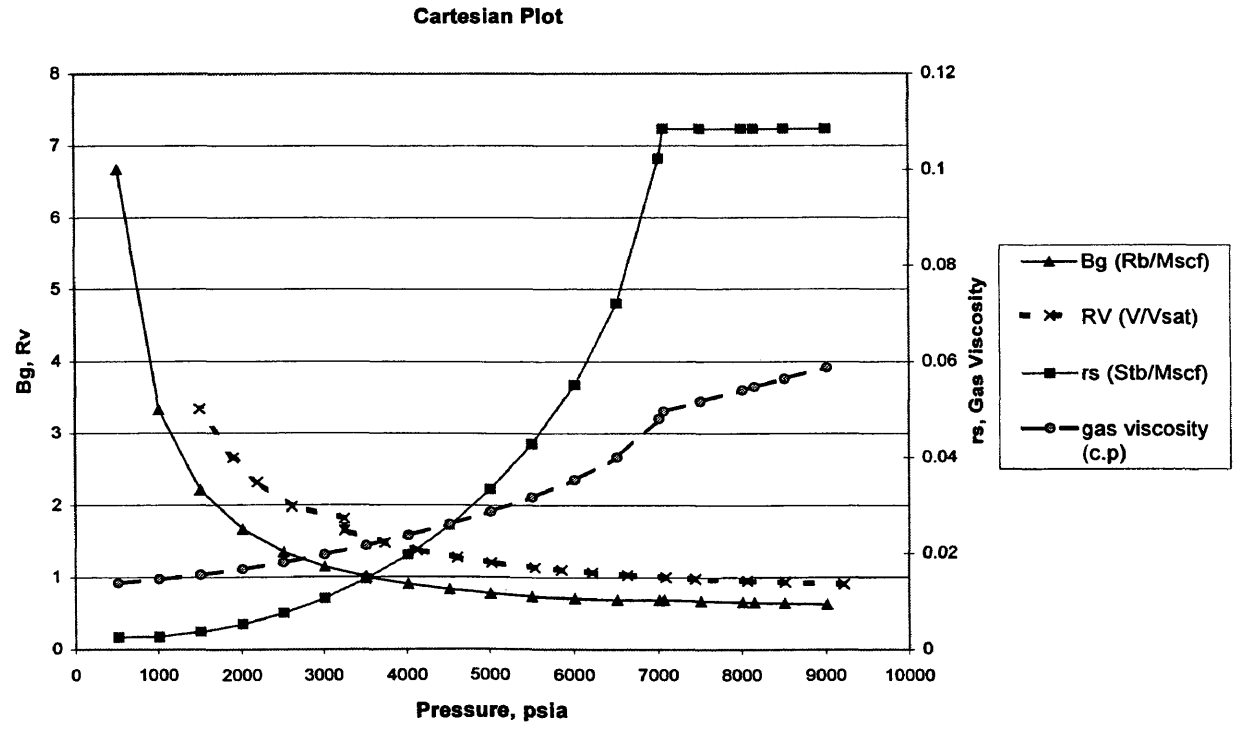

Fig. 2.8 Gas Property data for test conducted on June 21, 1998.

Water property data (PVTW) were calculated using the petroleum fluids toolkit[10] and the Brigham and Standing correlations. **Table 2.7** shows the properties of the water.

Table 2.7

Water Property Data

Reference Pressure **P** **(psia)**	**Water Viscosity** μ_w **(c.p)**	**Water Compressibility** C_w **(1/psia)**	**Gas Soluble in Water** R_{sw} **(scf/bbl)**	**Water Formation Factor** B_w **(bbl/stb)**
8102.65	0.29148	$2.95*10^{-6}$	15	1.053

2.4 RELATIVE PERMEABILITY AND CAPILLARY PRESSURE

The Honarpour, et al.[4] (1982) correlation was used to construct relative permeability curves because laboratory data were not available. The Honarpour, et al. equations depend on rock type and the formation wettability. In this project, the correlation for sandstone was used. The correlations used to generate the relative permeability data in this study are presented below as a function of wettability and lithology.

Water-wet sandstone:

$$k_{rw} = 0.035388\left(\frac{S_w - S_{wi}}{1 - S_{wi} - S_{orw}}\right) - 0.010874\left(\frac{S_w - S_{orw}}{1 - S_{wi} - S_{orw}}\right)^{2.9} + 0.56556(S_w)^{3.6}(S_w - S_{wi}) \ldots.(2.5)$$

Sandstone with any wettability:

$$k_{row} = 0.76067\left(\frac{\left(\frac{S_o}{1 - S_{wi}}\right) - S_{orw}}{1 - S_{orw}}\right)^{1.8}\left(\frac{S_o - S_{orw}}{1 - S_{wi} - S_{orw}}\right)^2 + 0.26318\phi(1 - S_{orw})(S_o - S_{orw}) \ldots(2.6)$$

$$k_{rog} = 0.98372\left(\frac{S_o}{1 - S_{wi}}\right)^4\left(\frac{S_o - S_{org}}{1 - S_{wi} - S_{org}}\right)^2 \ldots\ldots\ldots(2.7)$$

$$k_{rg} = 1.1072\left(\frac{S_g - S_{gc}}{1 - S_{wi}}\right)^2 k_{rg(S_{org})} + 2.7794\left(\frac{S_{org}(S_g - S_{gc})}{1 - S_{wi}}\right) k_{rg(S_{org})} \ldots\ldots\ldots(2.8)$$

where

ϕ = porosity

S_{wi} = irreducible water saturation

S_{gc} = critical gas saturation

S_{orw} = residual oil saturation in water-oil system

S_{org} = residual oil saturation in gas-oil system

k_{rw} = relative permeability to water

k_{rg} = relative permeability to gas

k_{row} = relative permeability to oil in water-oil system

k_{rog} = relative permeability to gas in oil-gas system

$k_{rg(Sorg)}$ = relative permeability to gas at residual oil saturation

The above equations were used to generate relative permeability tables[11]. The output file (ezgen.ecl) was used as starting point for building the Eclipse data file. Capillary pressure data were not available. Therefore, it is assumed to be zero and implies that there is no transition zone. The gas and water relative permeabilities k_{rg} and k_{rw} are needed for the well test history match. Oil relative permeability k_{ro} is needed for prediction runs when pressure drops below dew point pressure.

The input parameters used to solve the Honarpour, et al. Equations are the following:

S_{wi} = 24.3% from logs assuming there is no aquifer.

S_{orw} = Unknown.

S_{org} = Unknown.

Critical gas saturation, S_{gc} = 3 % assumed; no measurements.

Porosity, ϕ = 29.8% from logs.

End point K_{rg} = 1 assumed.

The figure below presents the calculated relative permeability curves for gas and water.

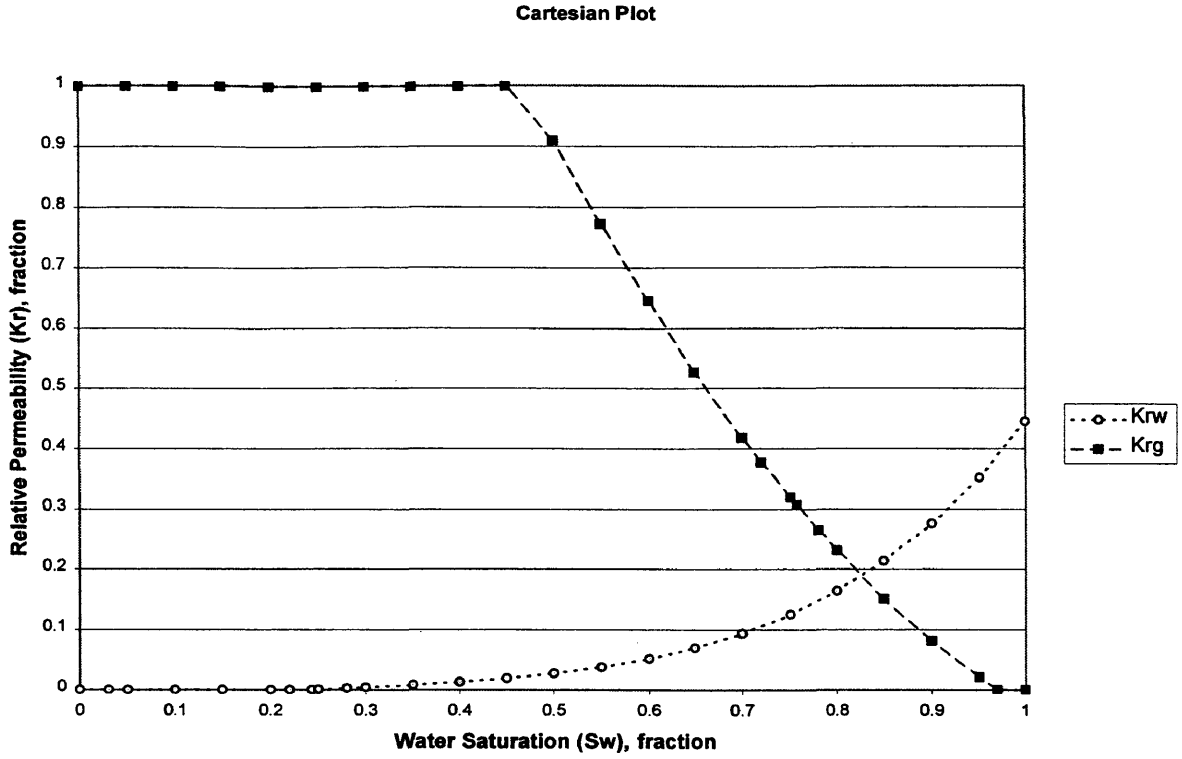

Fig. 2.9 Relative permeability curves.

2.5 INITIAL SATURATION AND PRESSURE DISTRIBUTIONS

The fluid properties discussed above imply that the reservoir is a gas condensate reservoir. The presence of an aquifer is inferred from the well log trace in **Fig. 2.2**. As long as the initial pressure is above the dew point pressure (7078 psig), there is only gas and water in the system. Condensate in the liquid phase will not appear until pressure is

below the dew point pressure. Gas-water contact (GWC) is found at around 10699′ as shown in **Fig. 2.2**. The datum pressure is set at the GWC and is approximately 8106 psia based on the static gradient obtained on June 23,1998 and shown in **Fig. 2.10**.

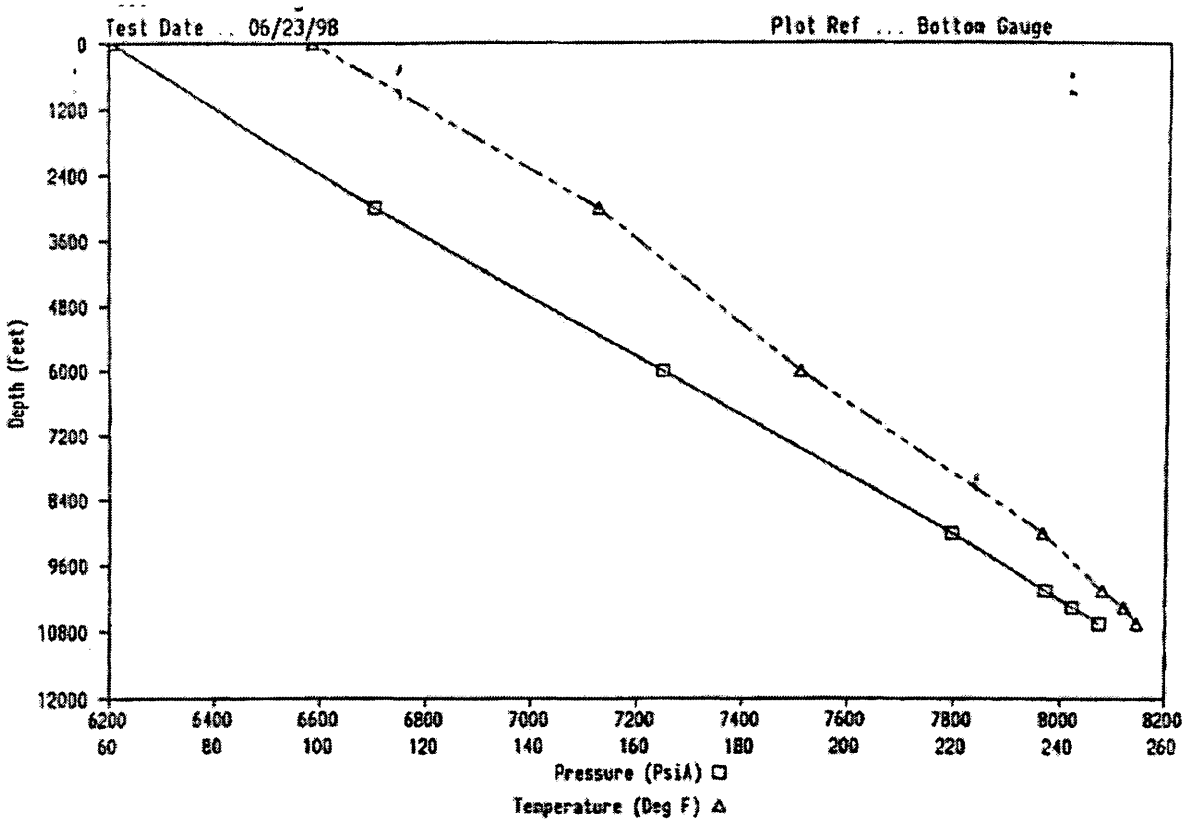

Fig. 2.10 Static pressure gradient obtained on June 23,1998.

2.6 ORIGINAL FLUIDS IN PLACE

The simulator provided a volumetric estimate of original fluids in place upon initialization. Simulator volumes show that the initial gas in place is approximately 99.45×10^3 MMscf of free gas and 10.79 MMstb of condensate gas (vaporized oil).

Chapter 3

HISTORY MATCH

The aim of a numerical model study is to obtain results with more accuracy than is possible with simpler techniques. Therefore, for a model to behave like a reservoir, it must be conceptually similar to the reservoir. This can be done by history matching. The most important task is to determine which data should be matched during the history matching process. Simulation studies are usually performed on reservoirs that have some period of historical performance. Historical data often includes WOR, GOR, individual and cumulative phase rates, and pressure measurements. Ideally, periodic, accurate measurements of all of these data would be recorded and available for all wells. In the typical case however, much of the desired data is unrecorded or unavailable, and some of the reported values may be of questionable accuracy.

History matching is like art because of the need to make subjective judgments to solve the problem. On the other hand, there are some general guidelines that can expedite the history matching process. These guidelines have been presented by such authors as Mattax and Dalton[1] and Crichlow [12]. One set of guidelines is shown below:

- Match volumetric parameters with material balance.
- Match the reservoir pressure.

- Match saturation dependent variables.
- Match well flowing pressures.

The pressure match is usually the first match to be sought during the history matching process. One way to evaluate the history match is to compare the observed and the calculated parameters by plotting pressure behavior using semi-log and Cartesian plots. Log-Log plot (Diagnostic plot) can give the best distinction and improves the ability to correctly identify the flow regimes. In this study, the history match is based on matching the pressure build-up test for Well #1. This may have some restrictions because of its short period and to the lack of geological information.

Two different build-up well test analyses were available, as shown in **Table 2.3**. The build-up test conducted on June 23, 1998 was the longest one available and conducted shortly after lab data were obtained from tests on samples taken June 21, 1998 as shown in **Table 2.4** and **Table 2.5**. This test was run for 24 hours after a production period of around 5 days. The actual pressure data are shown in semi-log plot **Fig. 3.1**. The plot displays a straight line at early data and curved line from middle to late of the data. A log-log plot of pressure data and its derivative is able to display many separate characteristics more clearly as shown in plot **Fig. 3.2**. The pressure derivatives are calculated using the following relation[13].

$$t\left(\frac{\partial p}{\partial t}\right) = \left(\frac{\partial p}{\partial \ln t}\right)_i$$

$$= \left[\frac{\ln(t_i/t_{i-k})\Delta p_{i+j}}{\ln(t_{i+j}/t_i)\ln(t_{i+j}/t_{i-k})} + \frac{\ln(t_{+ji}t_{i-k}/t_i^2)\Delta p_i}{\ln(t_{i+j}/t_i)\ln(t_i/t_{i-k})} - \frac{\ln(t_{i+j}/t_i)\Delta p_{i-k}}{\ln(t_i/t_{i-k})\ln(t_{i+j}/t_{i-k})}\right] \quad \text{.....(3.1)}$$

$$\ln t_{i+j} - \ln t_i \geq 0.2 \quad \text{.....(3.2)}$$

$$\ln t_i - \ln t_{i-k} \geq 0.2 \quad \text{.....(3.3)}$$

where Δp = shut-in pressure and t = shut-in time.

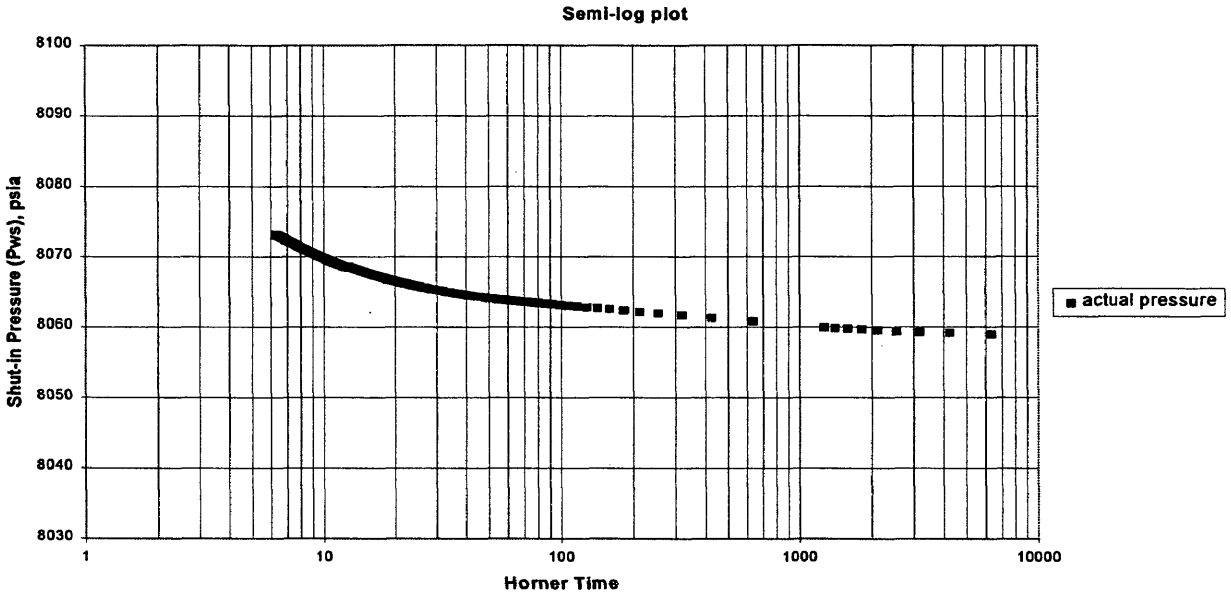

Fig. 3.1 Pressure behavior of June 23, 1998 data.

The diagnostic (log-log) plot shows different flow regimes: strange early behavior which maybe due to short infinite acting radial flow ends at shut-in time = 0.05 hour followed by transition flow period that ends at shut-in time = 0.2. A boundary effect region follows the transition flow period. Another transition flow period starts at shut-in time = 2 hours before the second boundary region started. This different flow regime behavior maybe due to the location of the well in a wedge-shaped region formed by faults

(see in **Fig. 2.1**). Charles, et al.[14] interpreted wedge-shaped reservoirs using pressure build-up responses by comparing the results from simulated finite element model studies.

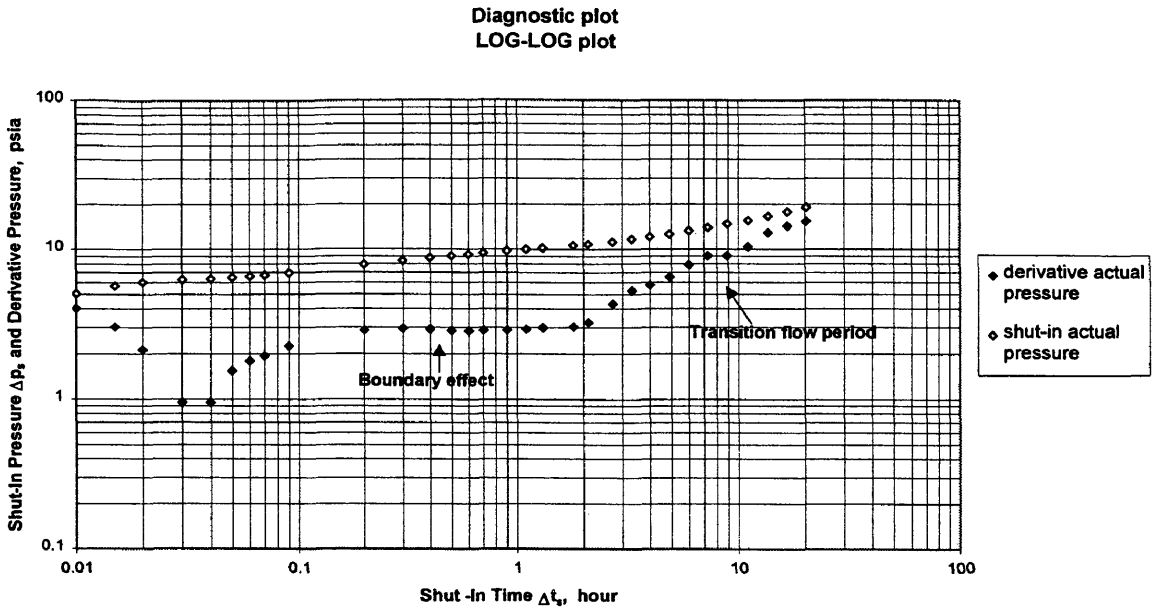

Fig. 3.2 Diagnostic plot of June 23, 1998 data.

Different models were run during the history match to find the best match of the build-up test data. Two different scenarios were developed based on the two different permeabilities obtained from the different tests.

The first model (initial case) was built using the available pressure data, and the saturation tables and PVT tables generated by the EZGEN and PVT software packages respectively. This model was run for a production period of 5 days and then a build-up of 24 hours. These periods are the same as the reported data. Results are shown in Cartesian plot **Fig. 3.3**. It is obvious that the initial case model needs to be modified to match historical pressure data.

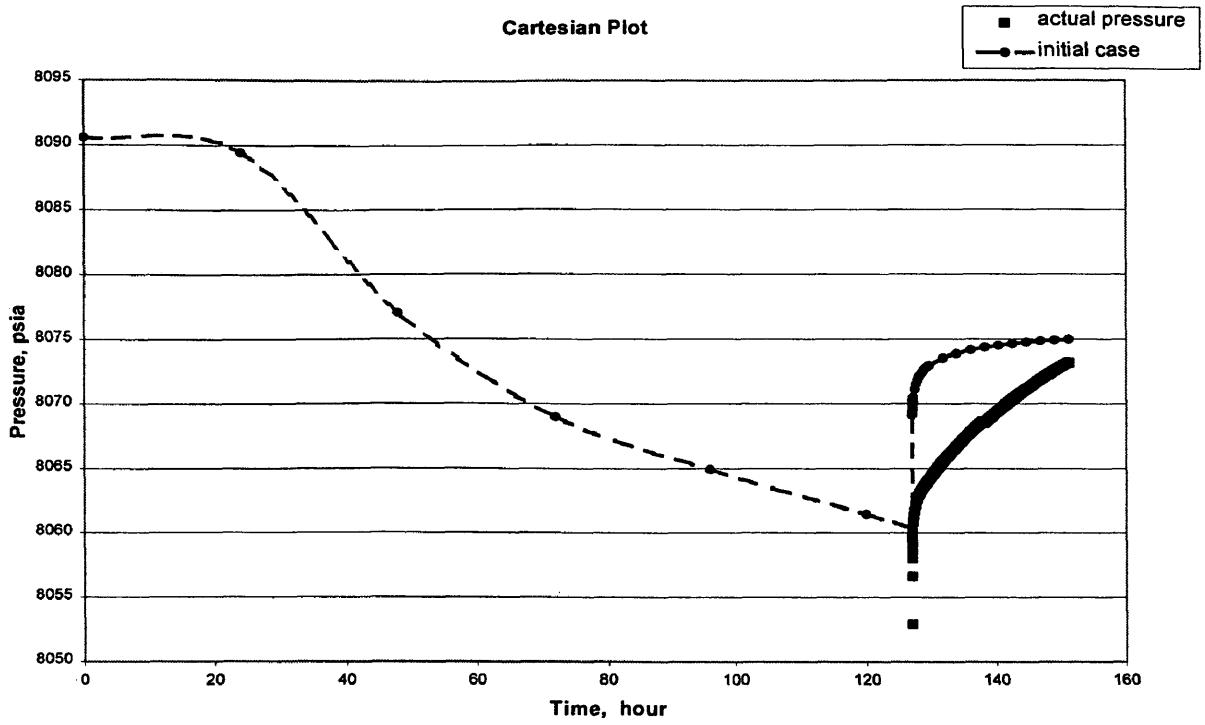

Fig. 3.3 Simulated and actual pressure data behavior for unmatched model.

The following information summarizes the data used in the base case model.

- Grid block dimensions:

  $NX = 26,\ \Delta X = 406'$

  $NY = 14,\ \Delta Y = 406'$

  $NZ = 5,\ \Delta Z_1 = 30',\ \Delta Z_2 = 36',\ \Delta Z_3 = 32',\ \Delta Z_4 = 10',\ \Delta Z_5 = 10'$

- Porosity:

  $\phi = 0.298$ for layers 2 and 4 (pay zone), and 5 (aquifer).

  $\phi = 0.0$ for layers 1 and 3 (non-perforated intervals).

- Datum pressure:

  P_{dat} = 8106 psia at depth of 10699′ (GWC).

- Production rates:

  Q_{g1} = 714 Mscf/d for 1 day.

  Q_{g2} = 7053 Mscf/d for 1 day

  Q_{g3} = 9536 Mscf/d for 1 day

  Q_{g4} = 9520 Mscf/d for 1 day

  Q_{g5} = 9303 Mscf/d for 1.3 days

  Q_{g6} = 0.0 Mscf/d for 1day

The 3D model used in this study is shown in **Fig. 3.4** below.

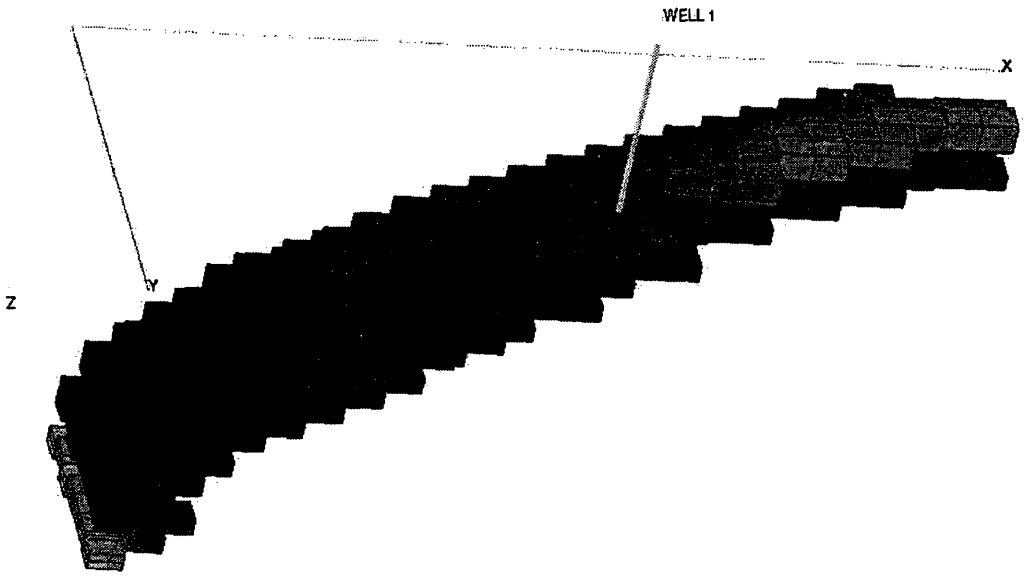

Fig. 3.4 3D model of the field.

3.1 FIRST SCENARIO

The permeabilities used in this scenario were obtained from the short build-up test during the infinite acting period shown in **Table. 2.3**. The permeabilities are:

$K_x = 665$ md.

$K_y = 665$md.

$K_z = 66.5$ md.

Vertical permeability was assumed to be one tenth of horizontal permeability, and horizontal permeability was assumed to be isotropic. These assumptions are tested by history match.

3.1.1 Initial Case.

The first model (initial case) was run and its results are shown in the semi-log plot **Fig. 3.5**. It is found that the simulated pressure has only one slope.

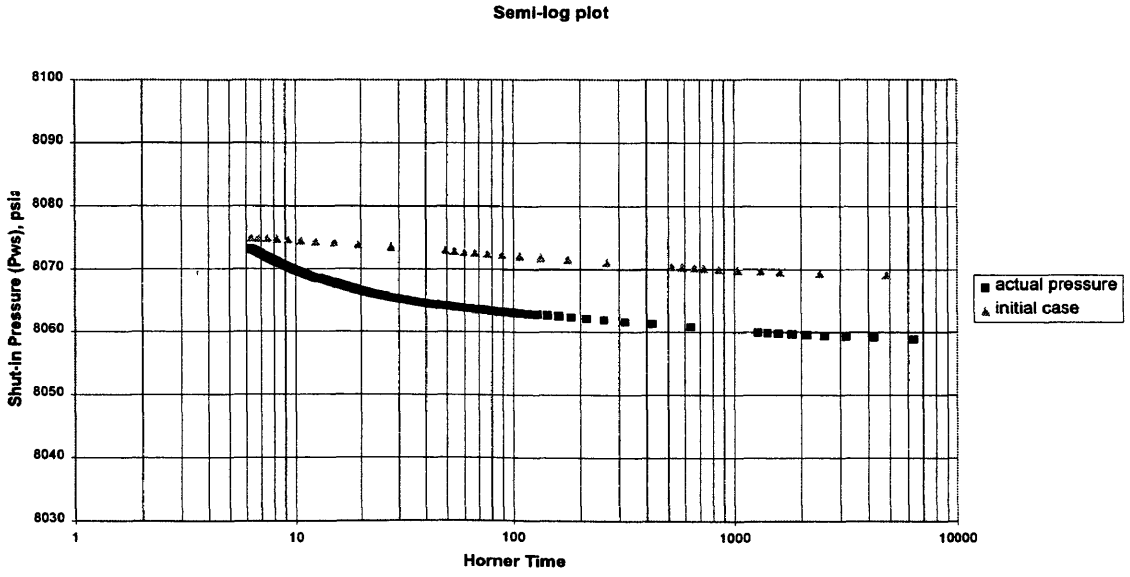

Fig. 3.5 Pressure behavior of the initial case model of first scenario

Therefore, runs with modifications were made to improve the history match.

3.1.2 Base Case.

Based on the sensitivity runs for the different models for the first scenario, it is found in the semi-log plot **Fig. 3.6** for the observed and the calculated pressure behavior that model case 5 (base case) gives the best match. On the other hand, it does not match the whole trend of the late time data and this is due to some restrictions with the matching pressure transient test. This model has a skin of 2 plus a minor seal fault (boundary) added to the north of Well #1 as a branch from the big southern seal fault II (**Fig. 2.1**) to form a wedge as shown in **Fig. 3.7**. It uses the following permabilities: Kx =665 md, Ky = 665 md., and Kz = 66.5 md. Transmissibility through the minor seal fault was reduced relative to the rest of the field by a factor MULTY = 0.

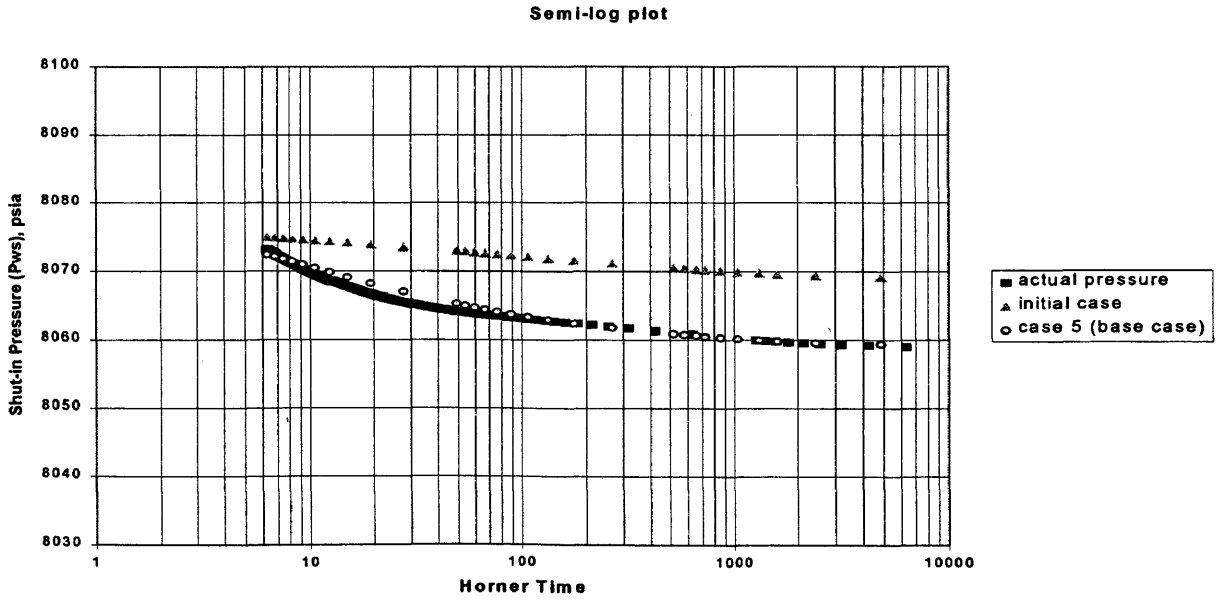

Fig. 3.6 Pressure behavior of initial and base case models of first scenario.

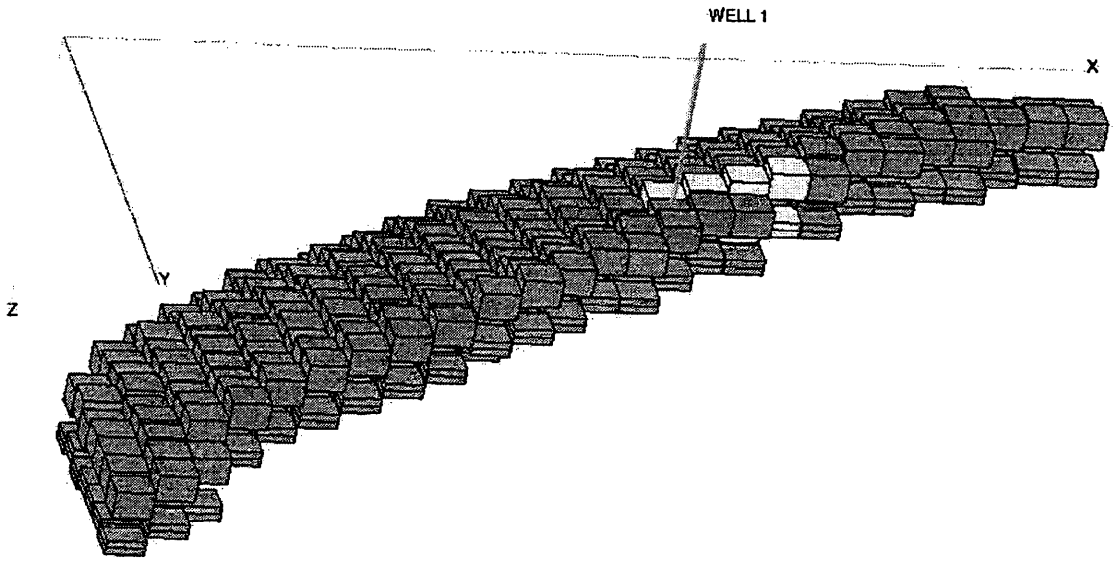

Fig. 3.7 3D model of the field representing minor seal fault added to the system.

There is a good chance that this minor seal fault shown in **Fig. 3.7** exists. It is not ruled out by seismic data, which was not available, and it is consistent with the geologic interpretation of seal faults in the reservoir. The flow regimes noted from the diagnostic plot show that the pressure responses sense two different boundaries because of the wedge-shaped reservoir. The well location near Fault II accounts for the short radial flow period shown in **Fig. 3.2,** the boundary effect is contributed to Fault II, and the long transition flow period is due to Fault I. The presence of the minor fault did significantly improve the match of pressure behavior shown in **Fig. 3.6** for a model of 665 md. The model permeability of 665 md. is consistent with the permeability obtained from the infinite-acting period obtained for matching the first test with a faulted boundary. This

result is reached by using the history match as an inverse problem. An inverse problem exists when the dependent variable is known and the independent variable must be determined. In this case, the pressure behavior is known by having radial and boundary effects, which is dependent on having another close boundary to the well or due to composite reservoir system. The composite reservoir due to phase changes is not expected because the pressure behavior to be matched was still above the dew point pressure of 7078psig. Changes in lithology could yield composite reservoir behavior.

3.1.3 Sensitivity Runs.

Different parameters and their effect on the history match are shown below for several sensitivity runs.

- Properties, Size and location of the seal fault effects

A seal fault was added to the north of the well with MULTY of zero in model case 1in order to form a wedge. The position and size of the fault were shown in **Fig. 3.7**. It can be seen in semi-log plot in **Fig. A.1** that the pressure is building enough in model case 1. Case 1 shows improvement in the match of the early data at large Horner times. The position of the fault is moved further north in model case 2. The position and the size of the seal fault are shown in **Fig. 3.8**.

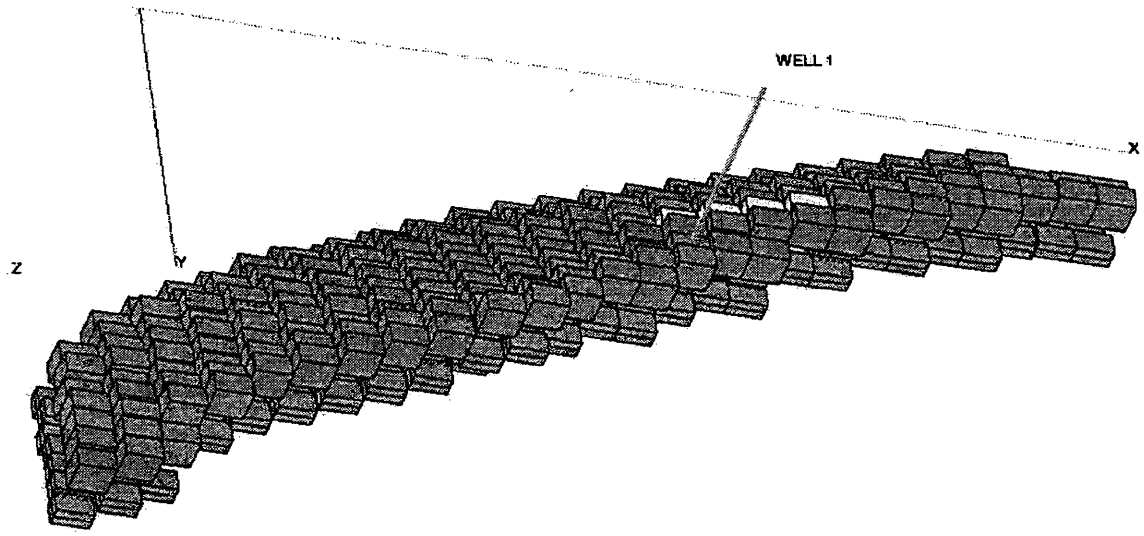

Fig. 3.8 3D model of the field representing new location of seal fault in model case 2.

This model shows higher pressure behavior than the real pressure as seen in **Fig. A.1**. Next, model case 3 was run with the same fault as case 1 but one property of the fault was changed by putting porosity equal to zero instead of putting MULTY equal to zero. This gives lower pressure behavior as shown in semi-log plot in **Fig. A.1**.

- Movement of the southern boundary effect

Next, model case 4 represents movement of the southern boundary adjacent to Well #1 of model case 1 half grid block to the south. It gives a little improvement in the match of middle to late data (small Horner time) compared to model case1, as shown in **Fig. A.2**.

- Skin effect

Model case 5 was run with a skin of 2 added in model case 4. There is little improvement in the early and middle data (large Horner time), as can be seen in the semi-log plot in **Fig. A.3.**

- Grid type effect

Local grid refinement using a radial grid method was done for the well block in model case 6, as shown in **Fig. 3.9.**

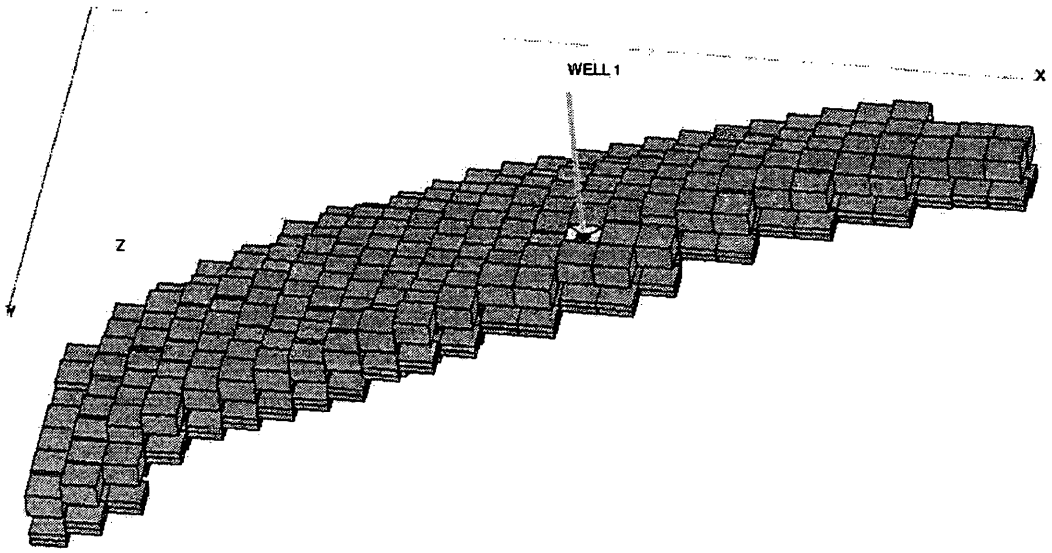

Fig. 3.9 3D model of the field representing radial grid refinement at well block.

Case 6 gives comparable pressure behavior as compared to case4 shown in **Fig. A.4.**

Another model case7 was run with a different local grid refinement (LGR) using a Cartesian grid system in the well block (**Fig. 3.10**).

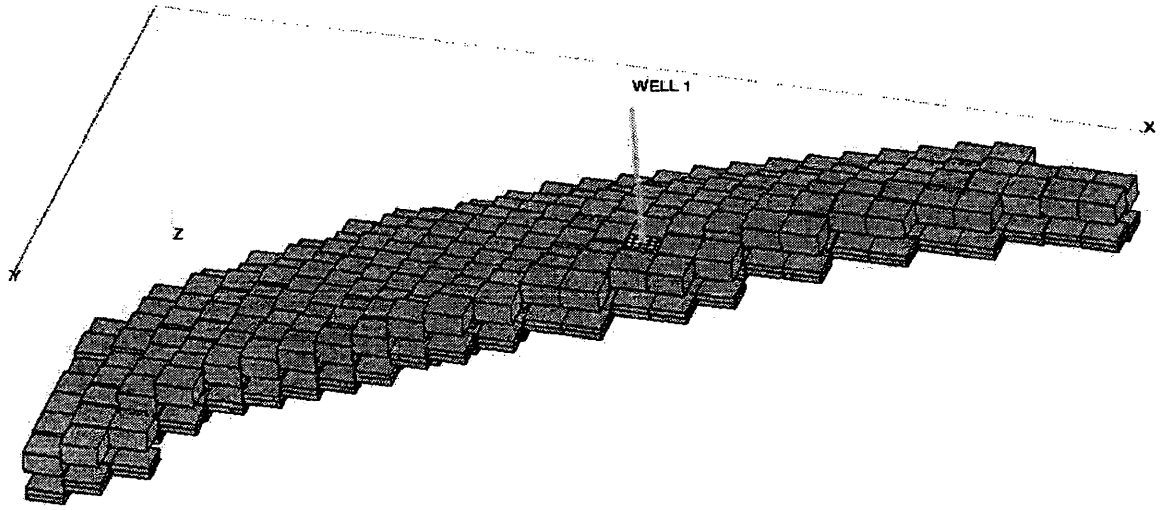

Fig. 3.10 3D model of the field representing the Cartesian grid refinement at well block.

It is found in **Fig. A.4** that the Cartesian grid refinement gives the same results as the radial system. The results of different grids are not significantly different, and indicate the Cartesian grid is adequately representing the reservoir under single phase production.

- Communication between layers effect

Model case 8 was run with porosities for the non-perforated layers (1 and 3) of model case 4 equal to the porosities for layers (2,4 and 5). The change in porosity increased the pay zone. The semi-log plot **Fig. A.5** shows higher pressure behavior for case 8 than for case 4. Therefore, model case 9 was run with changing the permeabilities

in z-direction of model case 8 for the layers (1 and 3) to zero to simulate impermeable shale barriers according to the lithology of the pay zone shown in **Table 2.1**. It can be seen in the semi-log plot in **Fig. A.5** that model case 9 gives similar behavior as model case4. This means that porosities or permeability in z-direction equal to zero both represent the flow barrier. Another model (case 10) was run with a reduction of the permeability in the x and y-directions of model case 9 from 665 to 520 md because of the existence of some shale in the bottom perforated interval. It can be seen in Semi-log plot **Fig. A.5** that there is no significant improvement in the matching compared to model case 4.

Based on the sensitivity runs for the different models for the first scenario, it can be seen in the semi-log plot in **Fig. 3.11** for the observed and the calculated pressure behavior that model case 5 gives the best match.

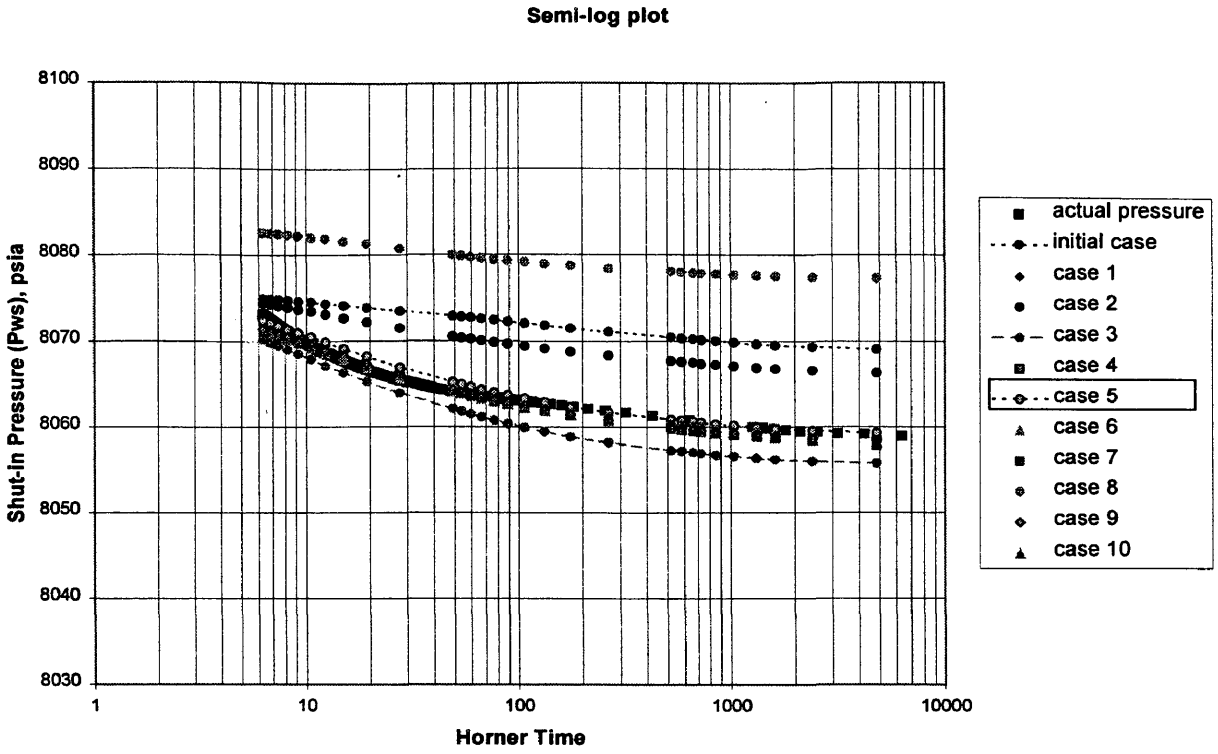

Fig. 3.11 Sensitivity runs of history matching of first scenario.

3.2 SECOND SCENARIO

The permeabilities used in this scenario were obtained from the long build-up test during the boundary effect period as shown in **Table. 2.3**. The permeabilities are:

$K_x = 229$ md.

$K_y = 229$ md.

$K_z = 22.9$ md.

Vertical permeability was assumed to be one tenth of horizontal permeability, and horizontal permeability was assumed to be isotropic. These assumptions are tested by history match.

3.2.1 Initial Case.

The first model (initial case) was run. It gave a good match of the actual pressures as shown in **Fig. 3.12**.

Runs with modifications were made in an attempt to improve the history match.

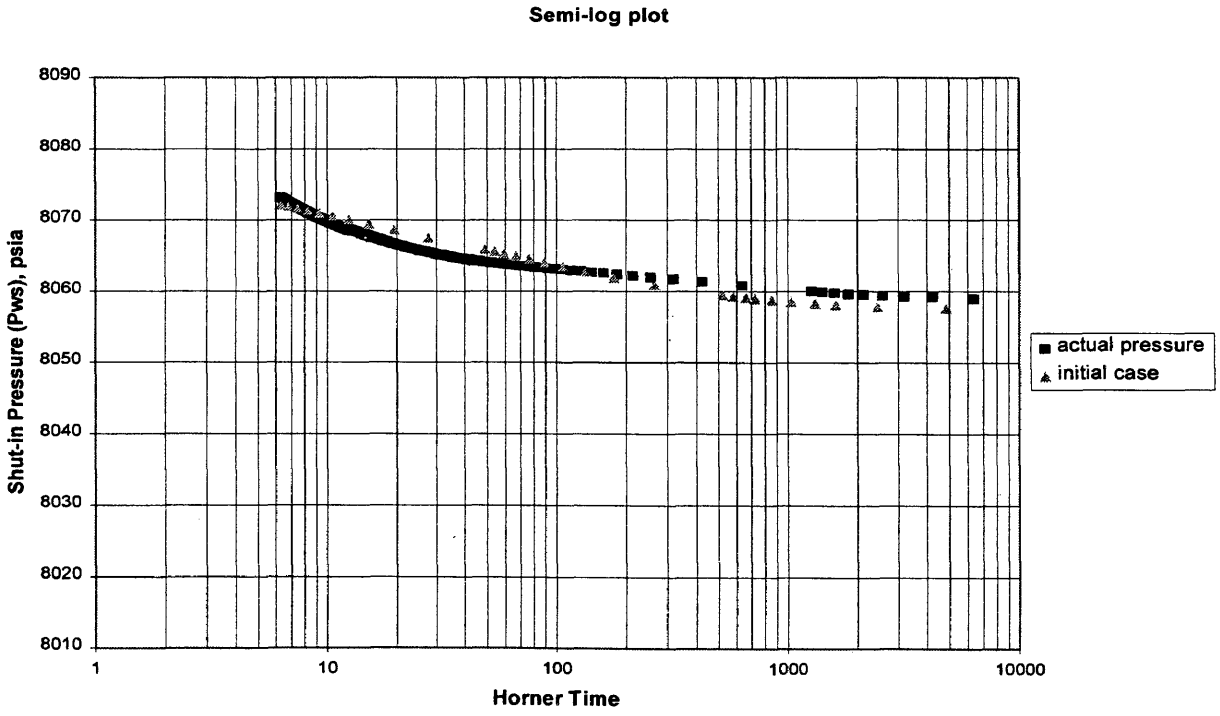

Fig. 3.12 Pressure behavior of the initial case model of second scenario.

3.2.2 Base Case.

Based on the runs for the different models for the second scenario, model case 1 is found to be the base case of the second scenario, as shown in **Fig. 3.13**.

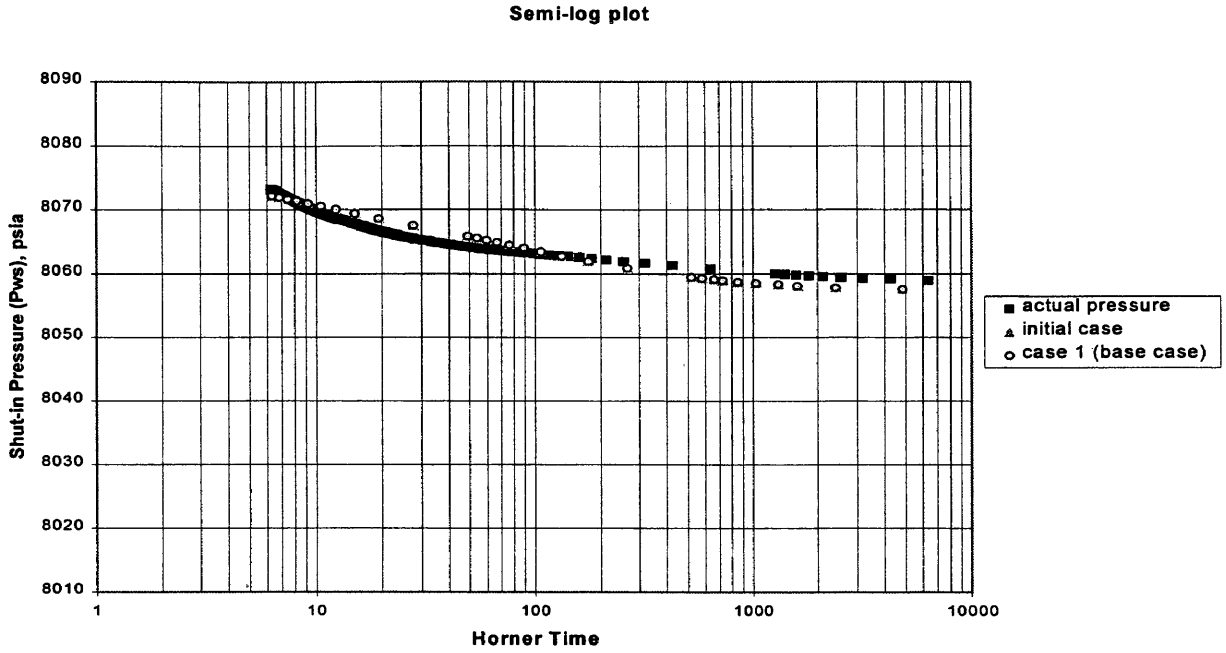

Fig. 3.13 Pressure behavior of initial and base case models of second scenario.

Case 1 has a porosity of 0.298 and permeability in z-direction between layers one and two and between layers three and four of zero. This is based on the presence of shale barrier in layers one and three.

3.2.3 Sensitivity Runs.

Different models were run with modified parameters to show the effect of parameter changes on the match.

- Communication between the layers

According to the data mentioned earlier in the model initialization, a shale barrier is found in layers one and three. Therefore, model case 1 was run with porosities of 0.298 and permeability in z-direction of zero for layers one and three. It gives same behavior as the initial case model where the porosities of layers one and three are zero as shown in **Fig. A.6**. Another model case 2 was run with reduction in the permeability in z-direction of model case 1 from 22.9 to 5 md. for layer four. This is done according to the presence of some shale in producing layer four. No improvement in the match was found as shown in **Fig. A.6**. The improvement in the match of the middle data was noticed by running model case 3 with changes to the permeabilities in the x and y-directions of case 1 from 229 to 120 md instead of changing the permeability in the z-direction. This can be seen in **Fig. A.6**.

- Minor seal fault added effect

Model case 4 was run by adding a minor seal fault to model case 1. The size and location of the fault is the same as the one used in case 4 of the first scenario (see **Fig. 3.7**). **Figure A.7** shows that case 4 does not match actual pressures.

Based on the sensitivity runs for the different models for the second scenario, it can be seen in the semi-log plot in **Fig. 3.14** for the observed and the calculated pressure behavior that model case 1 gives the best match.

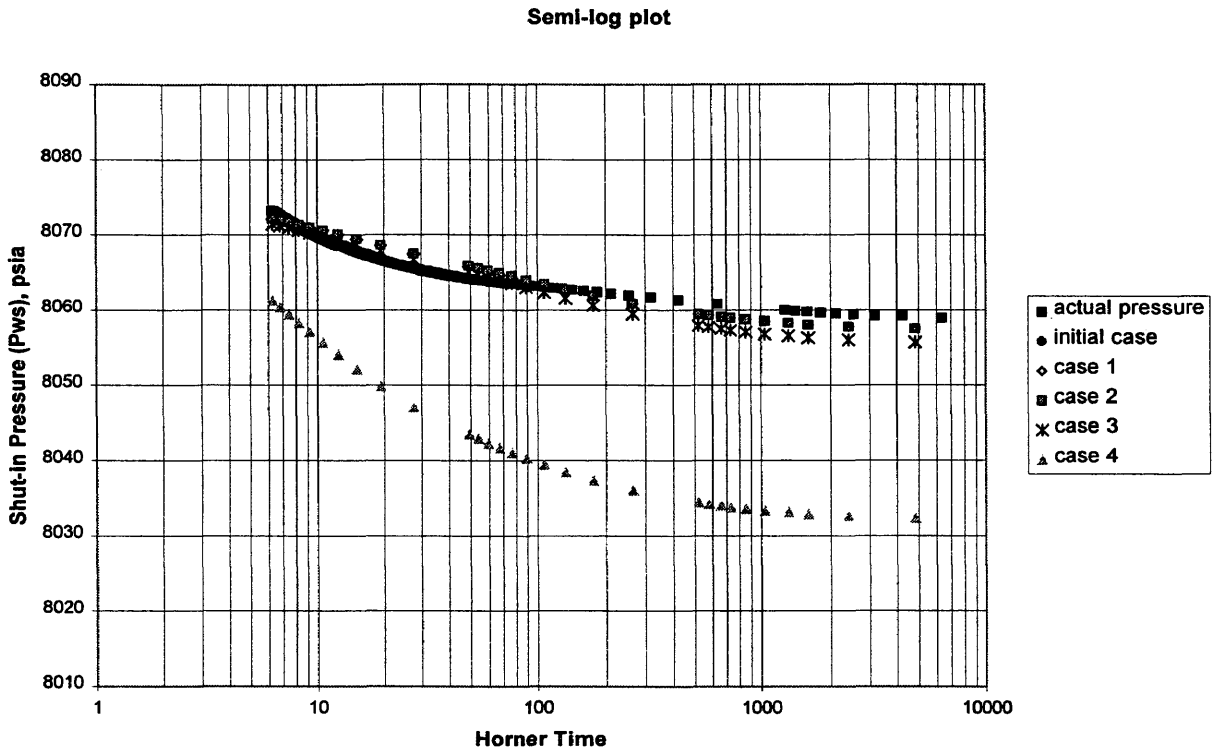

Fig. 3.14 Sensitivity runs for history matching of second scenario.

Model case 4 failed to match pressure data when a minor seal fault was added. This is because the permeability used in this scenario is low compared to the first scenario. Recall that the first scenario permeability was from the long test for a faulted boundary region. Therefore, the low permeability used in the second scenario has

accounted for the fault and there is no need to add a minor fault. According to Charles, et al.[14], it is possible that this low permeability is underestimated because of partial penetration effects.

Both scenarios are viable, alternative representations of the well test data. They show the non-unique character of the history matching process.

Chapter 4

PREDICTIONS

Running the predictions is the most interesting part of a simulation study and valuable for a variety of purposes, even though the actual running of predictions is usually the last phase of a simulation study. It provides the means of determining model sensitivity to changes in input data. Prediction runs give the future performance of the well or reservoir under different operating conditions. It consists mainly of two main parts.

4.1 BASE CASE

The first step is to prepare the base case prediction. This is a forecast using existing operating conditions. In this study, the best match found from the first scenario (case 5) was chosen as the base case model. This model was run for 100 days after the end of the history match period for the base case prediction. It is shown in **Fig. 4.1** that the rate of pressure decline does not change much as pressure drops below the dew point pressure (7078 psig). This indicates that the compressibility of the system does not change significantly when a small volume of condensate appears. **Figure 4.1** shows the increase in oil saturation as liquid drops out of the gas phase in the two-phase region

below the dew pint pressure. The oil saturation in the reservoir represents liquid or oil condensation.

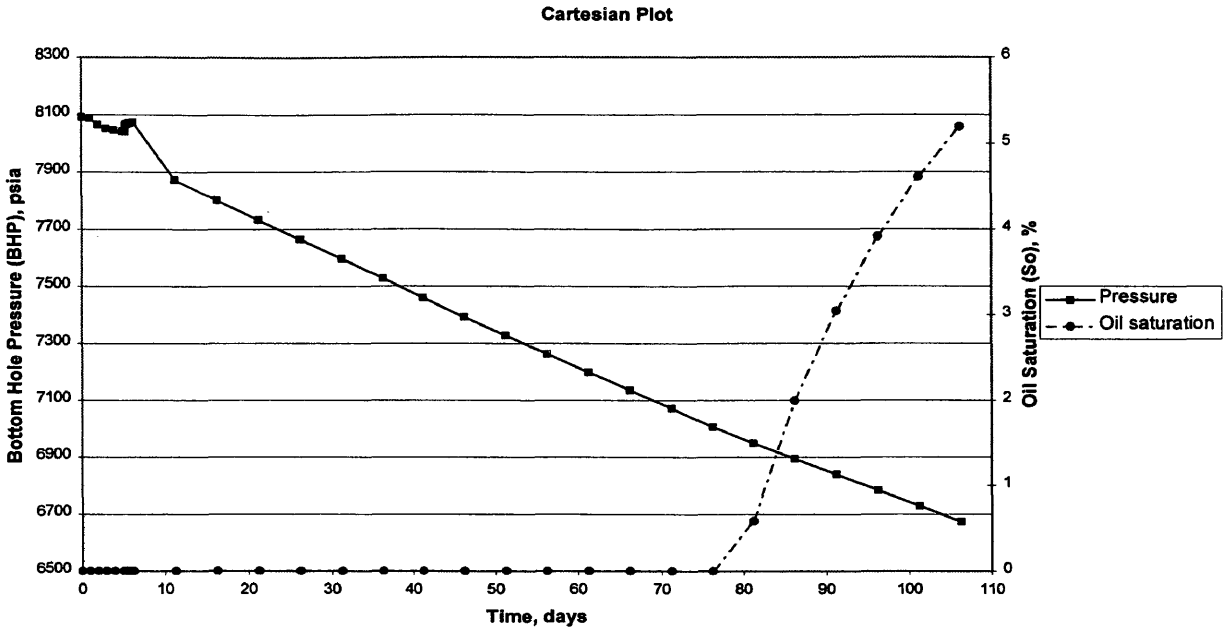

Fig. 4.1 Prediction run for base case model.

4.2 SENSITIVITY STUDY

Sensitivity cases are used to evaluate the changes of behavior for different values of key reservoir or operating parameters. These cases are valuable to assess the impact of major uncertainties on predicted performance. In this study, prediction sensitivity runs

were made to evaluate model performance for different types of grid systems and different gas relative permeability curves.

- Different type of grid system effect

The base case model was run with two different local grid refinement (LGR) options. They are Radial and Cartesian local grid refinement (LGR). It can be seen in **Fig. A.8** that the pressure behavior of both LGR methods is the same until it reaches the dew point pressure. At this point, the Radial LGR model has a lower pressure than the base case model. On the other hand, the Cartesian model gives the same pressure behavior as the base case until it reaches 6800 psia. The Radial LGR model has a larger oil saturation in the well block.

- Different gas relative permeability effect

Sensitivity cases were run with different gas relative permeability curves. There are four different cases for different critical gas saturation values: S_{gc} = 2%, 5%, 10% and 20%. The base case model has S_{gc} = 3% (see **Fig. 4.2**).

The prediction runs for the different relative permeability curves can be seen in **Fig. A.9**. This Figure shows that the shape of K_{rg} has a slight effect of pressure behavior. Curves with S_{gc} > 3% have lower pressures than the base case model with S_{gc} = 3%.

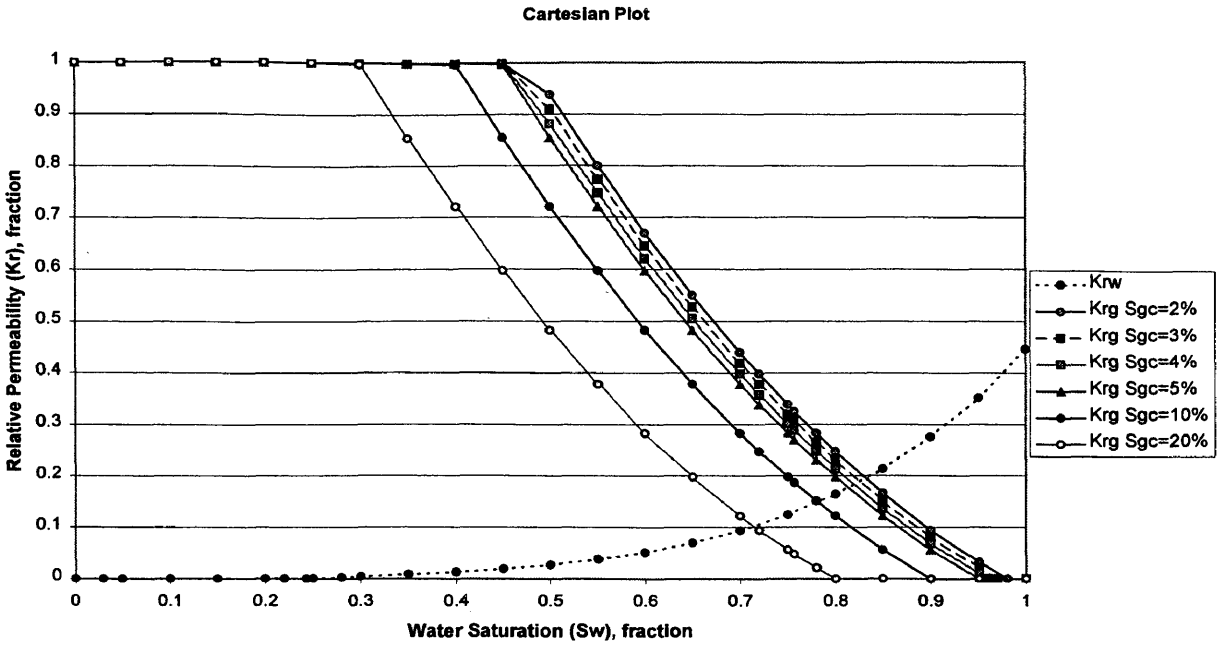

Fig. 4.2 Different gas relative permeability curves for different critical gas saturations.

Chapter 5

CONCLUSIONS & RECOMMENDATIONS

5.1 CONCLUSIONS

The objectives of the study have been met by initializing and building the model, obtaining a match of the data and making prediction runs for the base case at different conditions. Based on the work done in this research, the following conclusions can be drawn.

From the model initialization, it is found that the Peng-Robinson EOS gives a very good match for the gas condensate laboratory data.

Based on the history match obtained in this study, it is found that matching the pressure transient test has some restrictions because of its short period. It is concluded that the length of the well test in a well can influence the history match. The model with the areal permeability (K=665 md.) of the shorter test (infinite acting period) gave a match different from the model with an areal permeability (K=229 md.) from the longer test (faulted period). In the first scenario, the base case has a single minor fault added to the north of the well. In the second scenario, there is no need for this fault. The simulated pressures are not building up during the late time period as fast as the well test data, and they do not match the trend of late time pressure data very well. The lack of geological

information and the relatively short duration of the test in the context of the wedge faulting make matching the pressure transient test difficult. It appears there may be a boundary that is not provided in the present reservoir description. The location and properties of the seal fault to form a wedge give different behavior and can affect the match (see **Fig. A.1**).

The effect of skin and communication between layers is shown in **Figs. A.3 and A.5**. Different local grid refinement (LGR) options at well block give comparable behavior for this model.

In the prediction runs, different gas relative permeability curves change the pressure behavior of the well during two-phase flow. The Radial LGR has a greater affect on model prediction than does Cartesian LGR during two-phase flow. It has larger oil saturation in the well block than does Cartesian LGR.

A general procedure for studying a gas condensate reservoir was provided in **Sec. 1.2**. The steps include:

- Problem definition.
- Data review and acquisition.
- Selection of approach.
- Model initialization.
- History matching.
- Predicting performance.

5.2 RECOMMENDATIONS

Ideally, a match of data would include a match of the magnitude of the data and a match of data trends. In this case, two scenarios provided a match of the data magnitude, but neither matched the data trend of the late time period. Further work is needed to match the data trend.

Based on this study, it is recommended that field data be collected and matched. A more accurate representation of the reservoir could be obtained by attempting to match field performance when two phases are flowing.

The presence of condensate in the wellbore during a flow test would make it possible to study a wider range of phenomena for multi-phase flow.

Fluid property data for Well #1 appear to show the presence of a compositional gradient. A compositional gradient study of the reservoir could be performed using existing PVT and compositional data for Well #1 from different depths.

REFERENCES

1. C. C. Mattax and R. L. Dalton, **Reservoir Simulation**, Richardson, Texas, 1990.
2. H. B. Bradley, **Petroleum Engineering Handbook**, Society of Petroleum Engineers, Richardson, Texas, 1987
3. J. R. Fanchi, **Applied Reservoir Simulation**, Houston, 1997.
4. K. Aziz and A. Settari, **Petroleum Reservoir Simulation**, (TN 871 A93), England, 1979.
5. P. E. Salisburg and J. M. Peden, Heriot-Watt U, "Compositional Two-Phase Vertical Lift Performance Modeling of Crude Oil and Retrograde Gas Condensate Wells", paper SPE 16925 presented at the 62nd Annual technical Conference of SPE, Dallas, September 27-30 1987.
6. S. A. Dmitrievsky, D. N. Bolotnik, D. V. Posvansky, G. G. Sarkisov, N. E. Schepkina, P. A. Yufin, I. U. Zaitcev and ONICS Oil and Gas Company, "Applying Modern 3D modeling Technology for a Large Gas Condensate Field in Pricaspian Basin", paper SPE 35529 presented at the 1996 European 3D Reservoir Modeling, Norway, April 16-17.
7. F. W Cole, **Reservoir Engineering Manual**, Houston, Texas, 1969.
8. G.A. Pope, W. Wu, G. Narayanaswamy, M. Delashed, M. Sharma and P. Wang, "Modeling Relative Permeability Effects in Gas Condensate Reservoirs", SPE49266

presented at SPE annual technical conference and exhibition, New Orleans, Louisiana, SEPT. 27-30, 1998.

9. T. Ahmed, **Hydrocarbon Phase Behavior**, Houston, Texas, 1989.
10. D. Muchmore, **Petroleum fluids Toolkit**, April, 1998.
11. J. R. Fanchi, "EZGEN", private communication, Golden, Co
12. H. B. Crichlow, **Modern Reservoir Engineering- A simulation Approach**, Englewood cliffs, NJ, 1977.
13. R. N. Horne, **Modern Well Test Analysis,** Palo Alto, California, May, 1995.
14. D. D. Charles, H. H. Rieke, and R. Purushothaman, "Well Test Characterization of Wedge-Shaped, Faulted Reservoirs", SPE 56685 presented at SPE annual technical conference and exhibition, Houston, Texas, OCT. 3-6, 1999.

APPENDIX A

FIGURE A.1

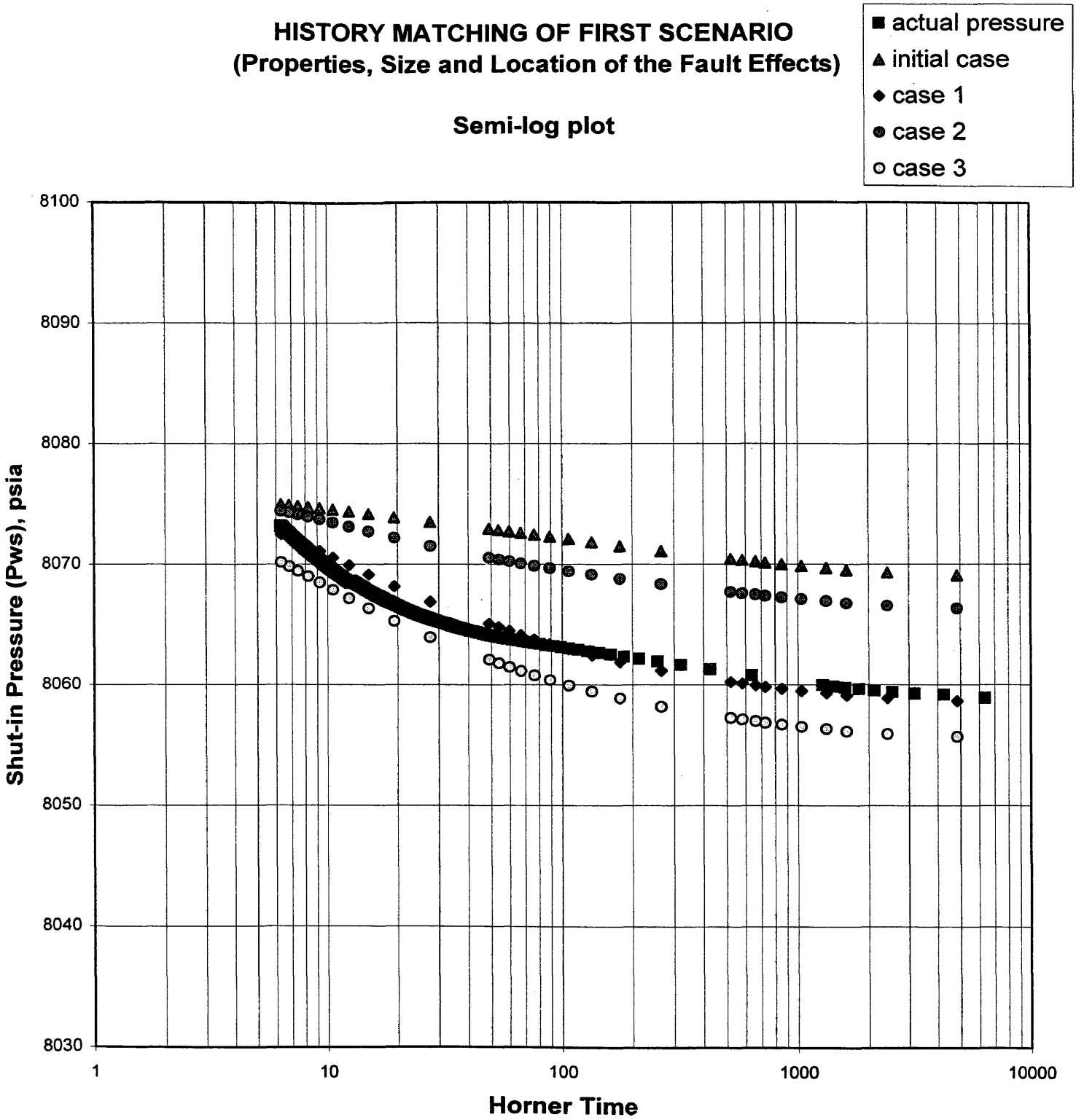
HISTORY MATCHING OF FIRST SCENARIO
(Properties, Size and Location of the Fault Effects)
Semi-log plot
actual pressure
initial case
case 1
case 2
case 3
Shut-in Pressure (Pws), psia
8100
8090
8080
8070
8060
8050
8040
8030
1
10
100
1000
10000
Horner Time

FIGURE A.2

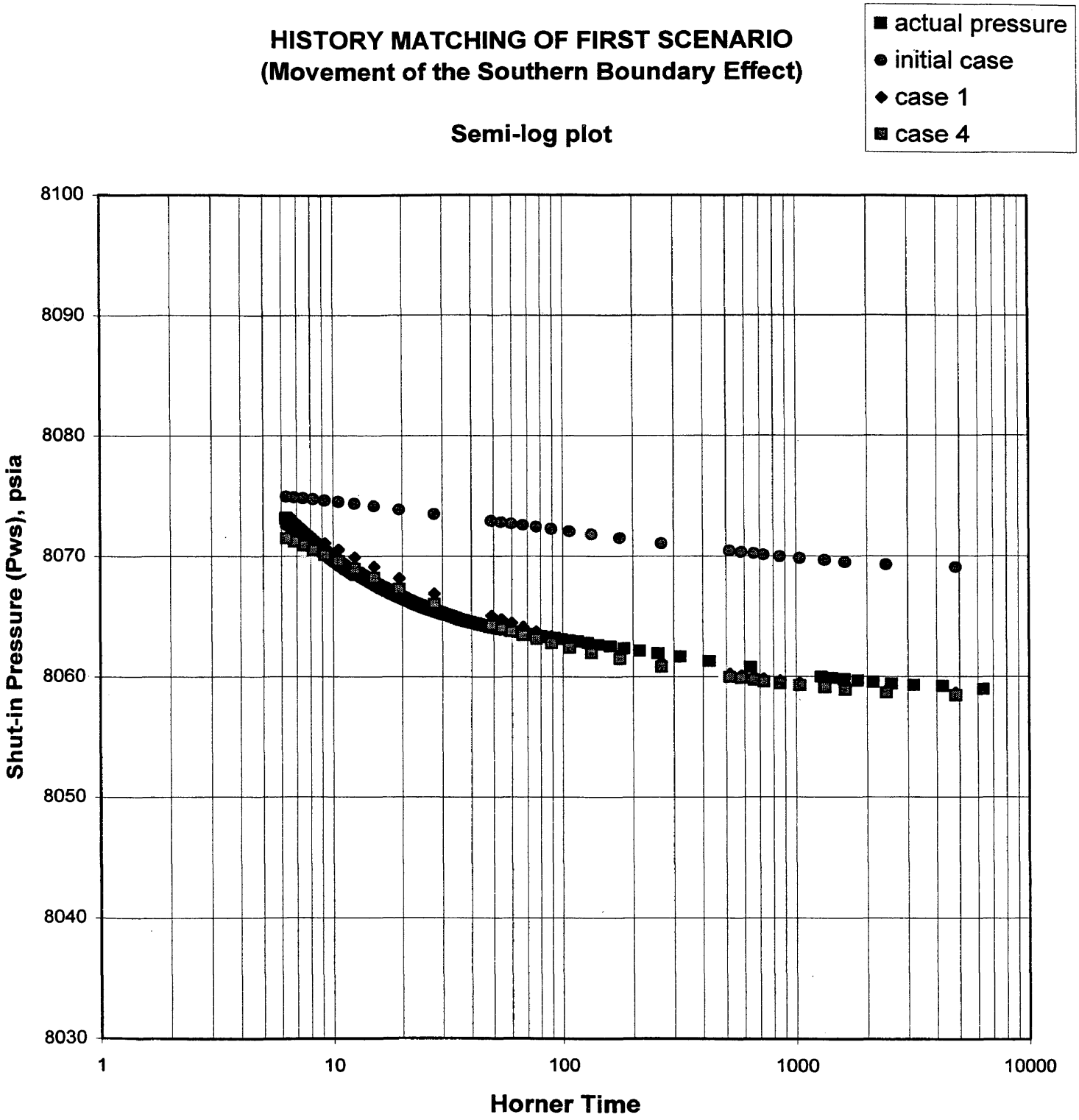
HISTORY MATCHING OF FIRST SCENARIO
(Movement of the Southern Boundary Effect)
Semi-log plot
actual pressure
initial case
case 1
case 4
8100
8090
8080
8070
8060
8050
8040
8030
Shut-in Pressure (Pws), psia
1
10
100
1000
10000
Horner Time

FIGURE A.3

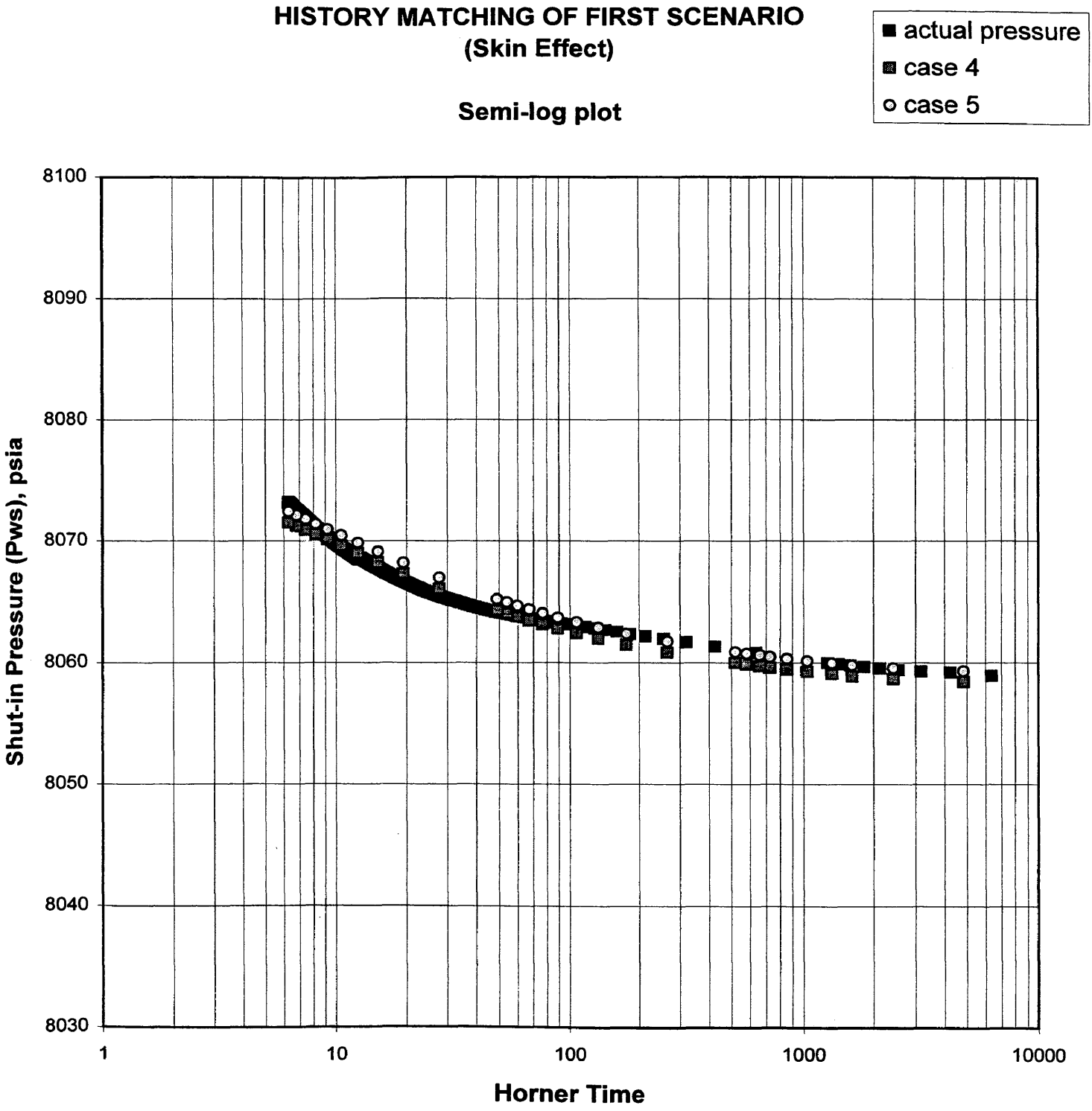
HISTORY MATCHING OF FIRST SCENARIO
(Skin Effect)
Semi-log plot
actual pressure
case 4
case 5
8100
8090
8080
8070
8060
8050
8040
8030
Shut-in Pressure (Pws), psia
1
10
100
1000
10000
Horner Time

FIGURE A.4

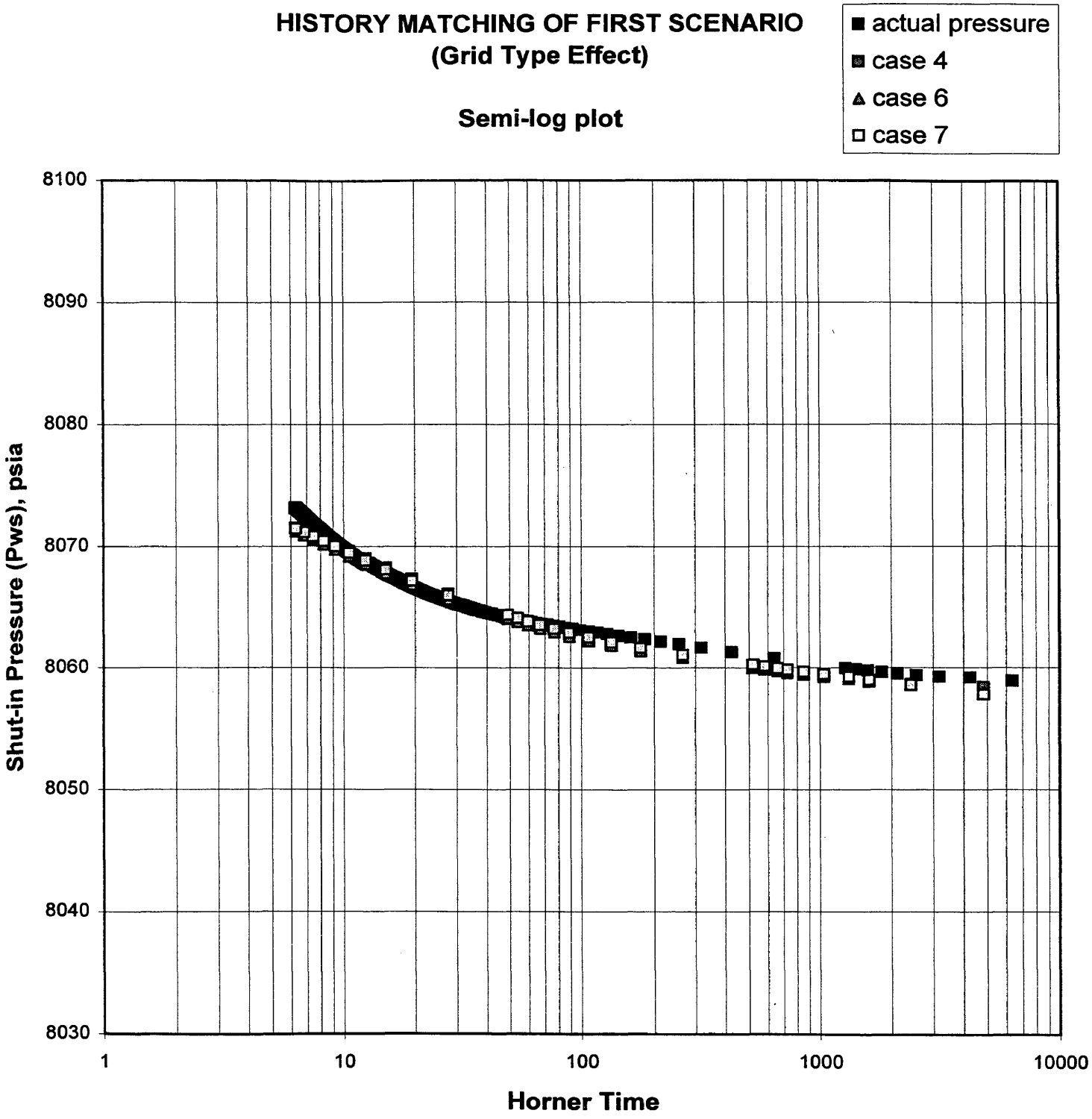
HISTORY MATCHING OF FIRST SCENARIO
(Grid Type Effect)
Semi-log plot
actual pressure
case 4
case 6
case 7
8100
8090
8080
8070
8060
8050
8040
8030
Shut-in Pressure (Pws), psia
1
10
100
1000
10000
Horner Time

FIGURE A.5

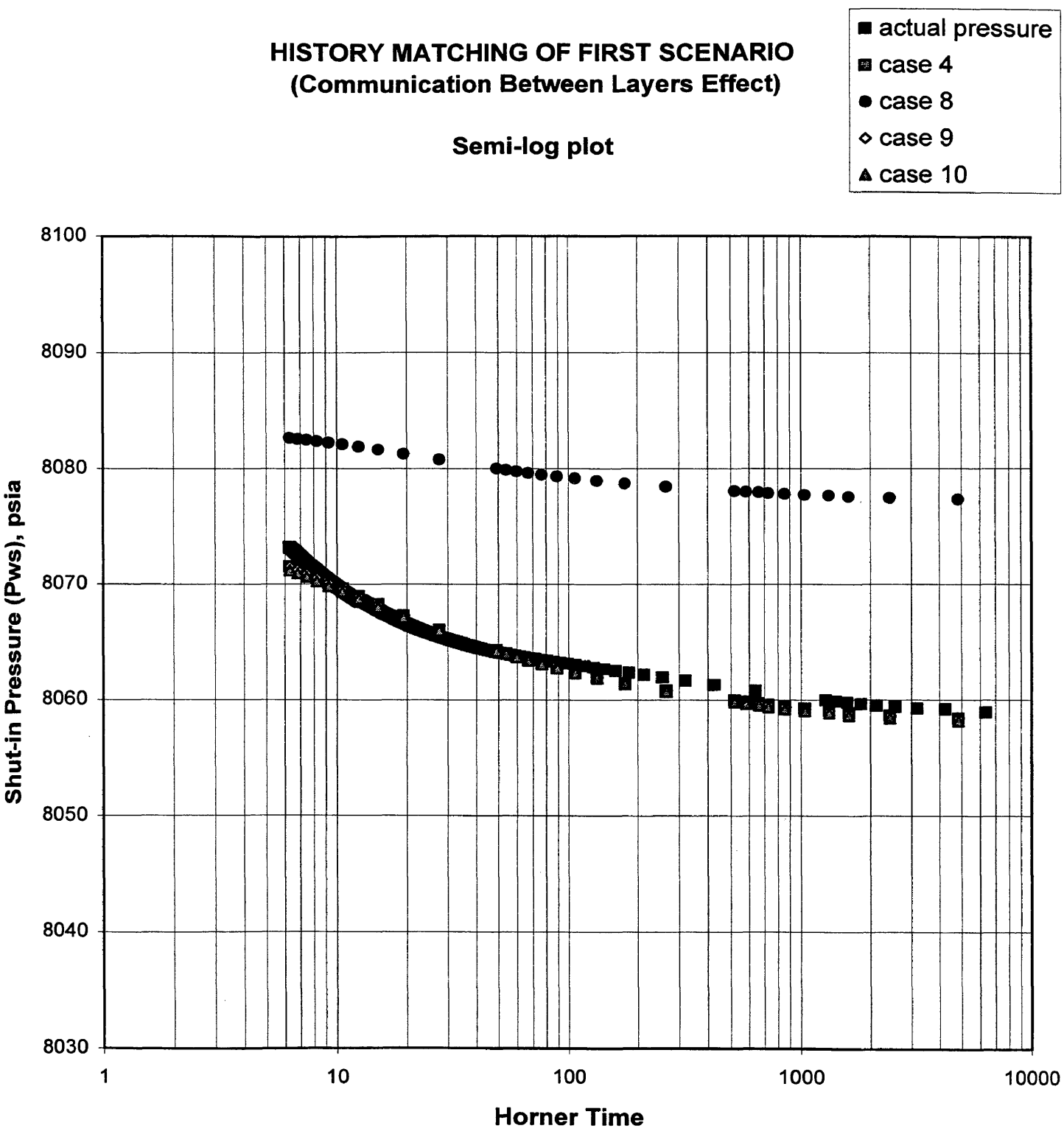
HISTORY MATCHING OF FIRST SCENARIO
(Communication Between Layers Effect)
Semi-log plot
actual pressure
case 4
case 8
case 9
case 10
Shut-in Pressure (Pws), psia
8100
8090
8080
8070
8060
8050
8040
8030
1
10
100
1000
10000
Horner Time

FIGURE A.6

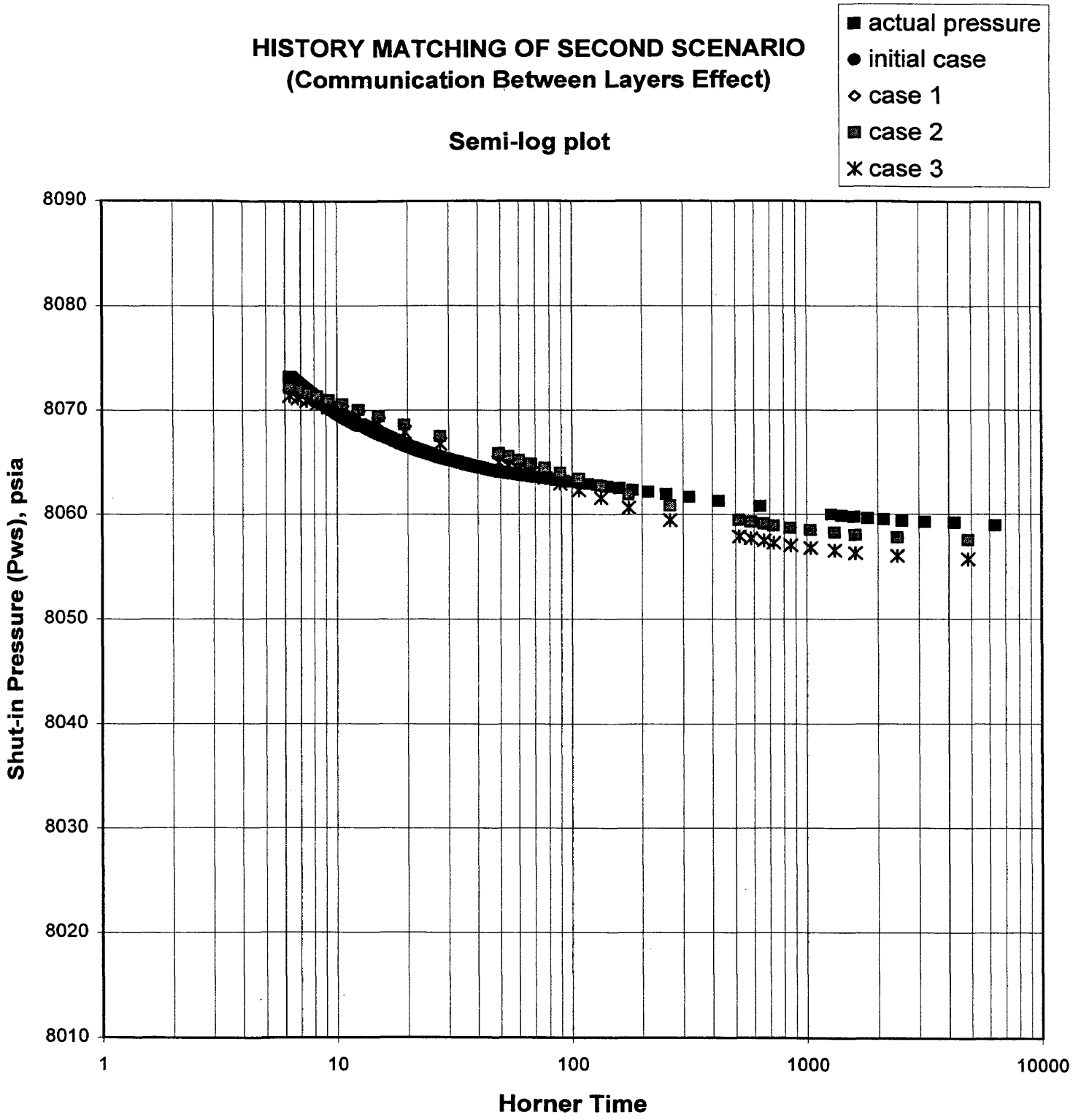
HISTORY MATCHING OF SECOND SCENARIO
(Communication Between Layers Effect)
Semi-log plot
actual pressure
initial case
case 1
case 2
case 3
Shut-in Pressure (Pws), psia
8090
8080
8070
8060
8050
8040
8030
8020
8010
1
10
100
1000
10000
Horner Time

FIGURE A.7

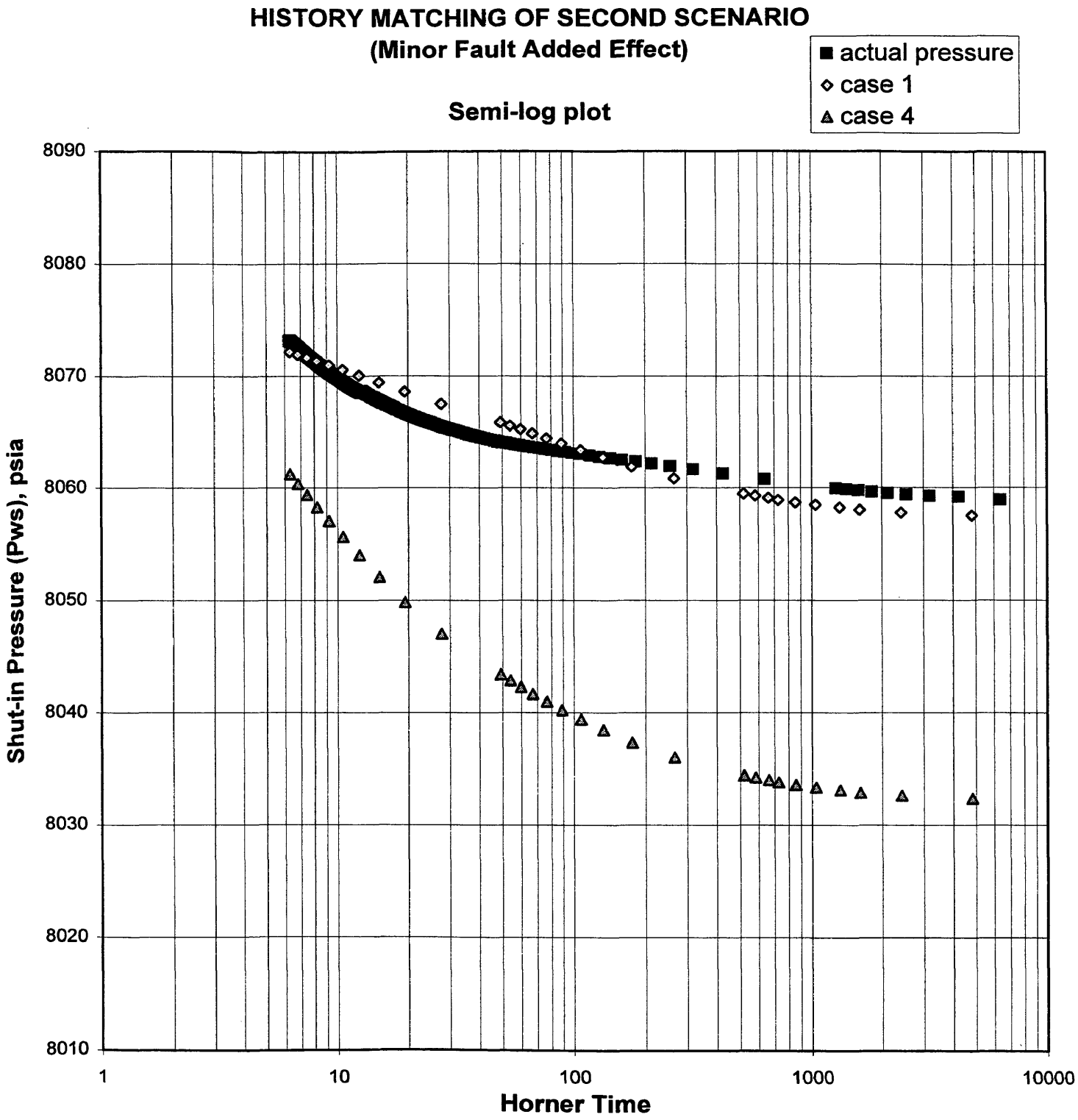
HISTORY MATCHING OF SECOND SCENARIO
(Minor Fault Added Effect)
Semi-log plot
actual pressure
case 1
case 4
Shut-in Pressure (Pws), psia
8090
8080
8070
8060
8050
8040
8030
8020
8010
1
10
100
1000
10000
Horner Time

FIGURE A.8

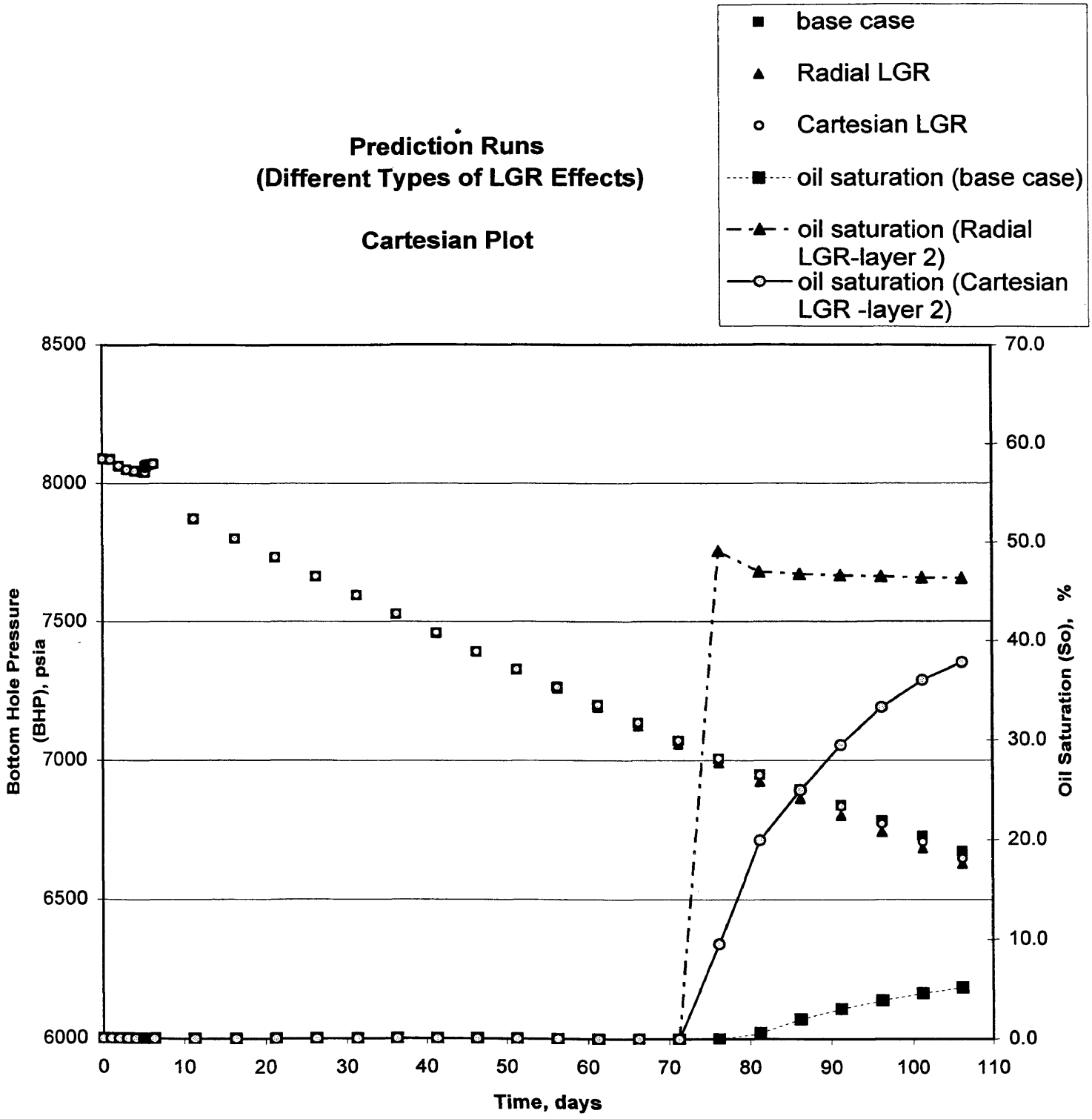
Prediction Runs
(Different Types of LGR Effects)
Cartesian Plot
base case
Radial LGR
Cartesian LGR
oil saturation (base case)
oil saturation (Radial LGR-layer 2)
oil saturation (Cartesian LGR -layer 2)
Bottom Hole Pressure (BHP), psia
Oil Saturation (So), %
Time, days
8500
8000
7500
7000
6500
6000
70.0
60.0
50.0
40.0
30.0
20.0
10.0
0.0
0
10
20
30
40
50
60
70
80
90
100
110

FIGURE A.9

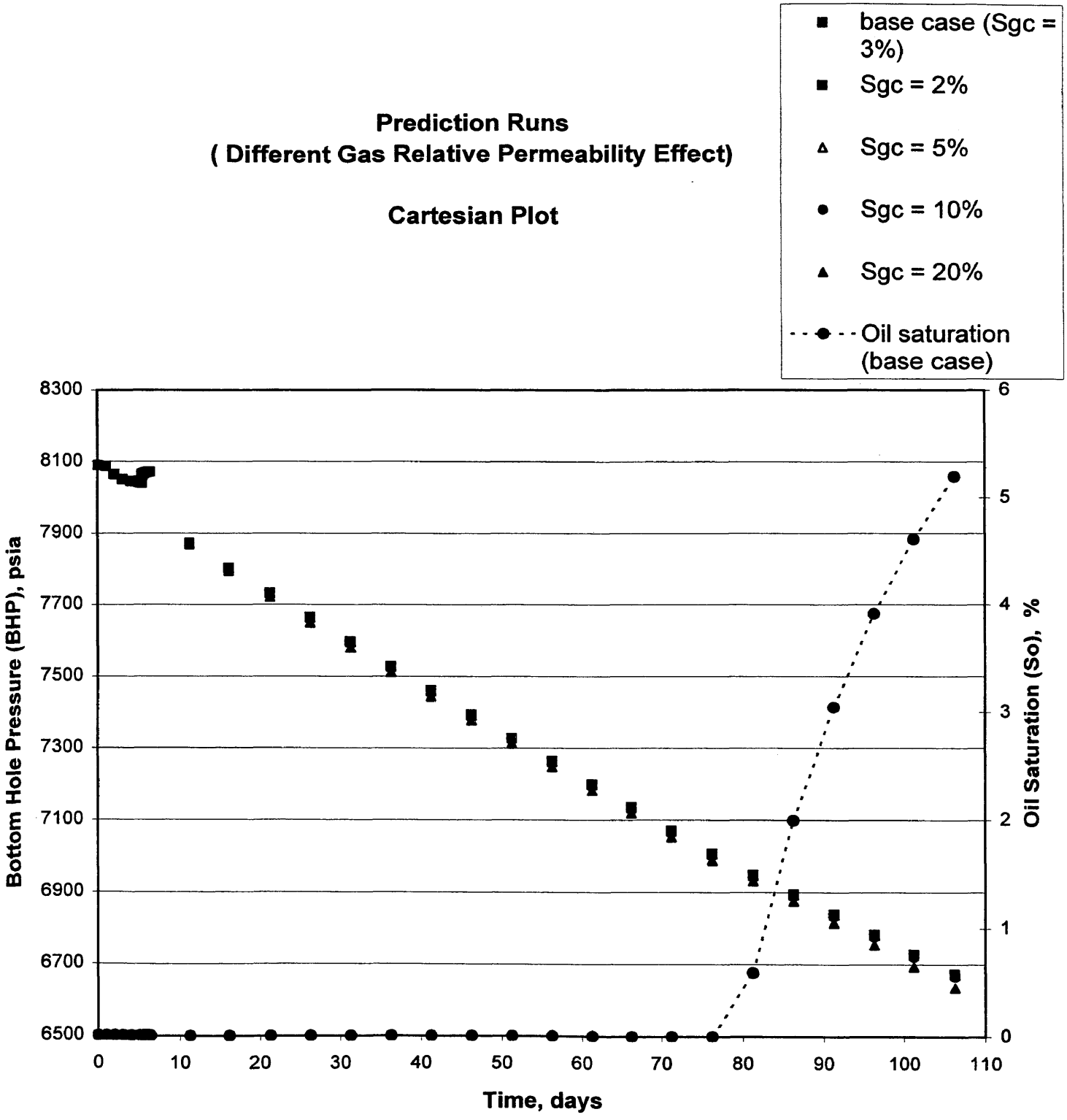
Prediction Runs
(Different Gas Relative Permeability Effect)
Cartesian Plot
base case (Sgc = 3%)
Sgc = 2%
Sgc = 5%
Sgc = 10%
Sgc = 20%
Oil saturation (base case)
Bottom Hole Pressure (BHP), psia
Oil Saturation (So), %
Time, days
8300
8100
7900
7700
7500
7300
7100
6900
6700
6500
6
5
4
3
2
1
0
0
10
20
30
40
50
60
70
80
90
100
110